ORGANOMETALLICS

pubs.acs.org/Organometallics

Article

Structural Diversity in the Reactions of Dimetallic Alkyl Titanium Oxides with Isonitriles and Nitriles

María Gómez-Pantoja, Juan I. González-Pérez, Avelino Martín, Miguel Mena, Cristina Santamaría,* and Manuel Temprado

Cite This: *Organometallics* 2021, 40, 2610−2623

Read Online

ACCESS | Metrics & More | Article Recommendations | Supporting Information

ABSTRACT: A detailed study of the reaction of the dinuclear $[\{Ti(\eta^5\text{-}C_5Me_5)R_2\}_2(\mu\text{-}O)]$ (R = Me **1**, CH_2Ph **2**) compounds with a series of organic isonitriles (R′NC, R′ = *t*Bu, *i*Pr, CH_2SiMe_3, Xyl) (Xyl = 2,6-$Me_2C_6H_3$) and nitriles (R′CN, R′ = *t*Bu, *i*Pr, $SiMe_3$) has been carried out. Single-crystal X-ray structural studies revealed a variety of reactivity and structural moieties. Theoretical calculations (density functional theory, DFT) were used to understand the mechanism of some uncommon reactions observed experimentally. Reactions of **1** and **2** with isocyanides *t*BuNC, *i*PrNC, and Me_3SiCH_2NC led to the formation of dimetallic η^2-iminoacyl species $[\{Ti(\eta^5\text{-}C_5Me_5)(R'NCR)R\}_2(\mu\text{-}O)]$ (R = Me, R′ = *t*Bu **3**, *i*Pr **4**, CH_2SiMe_3 **5**; R = CH_2Ph, R′ = CH_2SiMe_3 **6**). Complex **4** underwent net rearrangements at room temperature to give the imido-vinylamido derivative $[Ti_2(\eta^5\text{-}C_5Me_5)_2(\mu\text{-}O)(\mu\text{-}NiPr)\{N(iPr)CMe{=}CMe_2\}Me]$ (**7**), whereas the reaction of complex **2** with XylNC rendered the N—C bond cleavage product $[\{Ti(\eta^5\text{-}C_5Me_5)(CH{=}CHPh)\}(\mu\text{-}O)(\mu\text{-}\kappa^2\text{-}N,C\text{—}N(MeC_6H_3)CH_2)\{Ti(\eta^5\text{-}C_5Me_5)\}]$ (**8**). The reactions of **1** with nitriles *t*BuCN and *i*PrCN gave the ketimido products $[\{Ti(\eta^5\text{-}C_5Me_5)Me(CN(Me)R')\}_2(\mu\text{-}O)]$ (R′ = *t*Bu **9**, *i*Pr **10**), whereas the analogous processes with **2** gave the alkenyl-imido complexes $[\{Ti(\eta^5\text{-}C_5Me_5)(CH_2Ph)_2\}(\mu\text{-}O)\{Ti(\eta^5\text{-}C_5Me_5)(=NC(R')=C(H)Ph)(NCR')\}]$ (R′ = *t*Bu **11**, *i*Pr **12**) with the concomitant coordination of a nitrile molecule. Complex **1** reacts with Me_3SiCN to afford the nitrile−isonitrile isomerization product $[\{Ti(\eta^5\text{-}C_5Me_5)Me_2\}(\mu\text{-}O)\{Ti(\eta^5\text{-}C_5Me_5)(\kappa^2\text{-}C,N\text{-}Me_2CNSiMe_3)(CNSiMe_3)\}]$ (**13**).

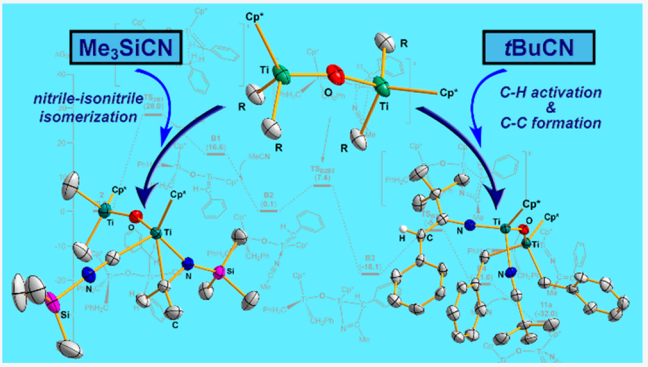

INTRODUCTION

Migratory insertion processes leading to the formation of iminoacyl (RC═NR) or ketimido (—N═CR_2) functionalities have received widespread attention. The isocyanide migration results in the formation of η^1- or η^2-iminoacyl species leading the metal nature. Early transition metals usually tend to favor the η^2-coordination, while low-oxidation-state metals (late transition metals, groups 8−10) tend to form η^1-iminacyl complexes. As compared to the insertion of isonitrile species, nitrile species (NCR) generally lead to ketimido products by 1,2-insertion processes (Scheme 1A). All of them comprise a standard methodology in which the generation of C−C bonds takes place, even into various metal−carbon bonds to give rise to multiple insertions.[1−4]

The resulting iminoacyl or ketimido complexes are able to undergo subsequent transformations in mild conditions. For instance, intramolecular coupling of bis(η^2-iminoacyl) group 4 or 5 metal complexes led to the formation of enediamido products.[2,5−12] Mild thermolysis involving initial coupling of η^2-imine and η^2-iminoacyl groups followed by fragmentation leads to the imido/alkenylamido functionalities,[13−16] or the rearrangement of a nitrile−ketimide species renders the

Scheme 1. Migratory Insertions of Nitriles and Isonitriles and Subsequent Transformations

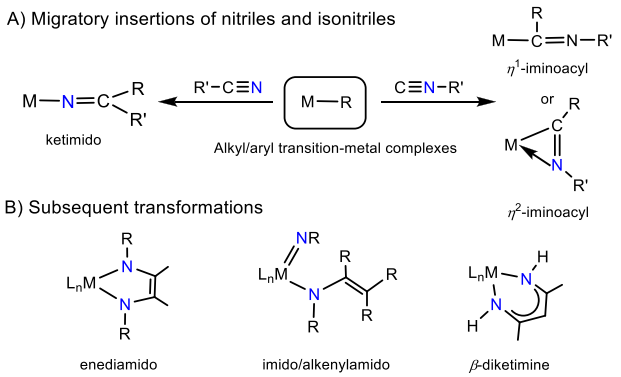

Received: May 19, 2021
Published: July 28, 2021

corresponding β-diketiminate products[17−19] (Scheme 1B). These reactions are important in the general context of the C−C and C−N bond forming processes, and this reactivity pattern mostly involves mononuclear transition-metal complexes, while only a few examples of di- or polynuclear species have been reported to date.[3,20−24]

It is expected that the cooperation of neighboring metals in multimetallic systems shows synergic effects, namely, new reactivity patterns, which cannot be achieved in monometallic species. This fact turned our attention to study the reactivity of the dinuclear alkyl titanium derivatives $[\{Ti(\eta^5\text{-}C_5Me_5)R_2\}_2(\mu\text{-}O)]$[25,26] (R = Me **1**, CH_2Ph **2**) with a series of isocyanides and nitriles. In this paper, we report situations in which an active cooperation between the metal centers takes place. The reaction mechanisms for some of these processes have been studied by DFT calculations.

RESULTS AND DISCUSSION

Reactions with Organic Isonitriles. The reactions of complexes $[\{Ti(\eta^5\text{-}C_5Me_5)R_2\}_2(\mu\text{-}O)]$ (R = Me **1**, CH_2Ph **2**) with some isonitriles are summarized in Schemes 2−4. The

Scheme 2. Reactions of Complexes 1 and 2 with Isonitriles

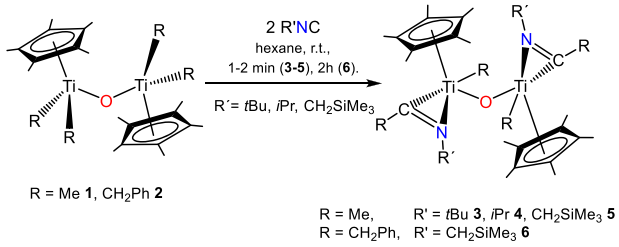

treatment of **1** with 2 equiv or an excess of R′NC (R′ = *t*Bu, *i*Pr, CH_2SiMe_3) in hexane, and cooling at −35 °C for a few days, afforded the η^2-iminoacyl complexes **3**−**5** in moderate−high yields (67−93%). The corresponding reactions of **2** were also carried out. While the treatment with *t*BuNC and *i*PrNC led to a complex mixture of products, the reaction with Me_3SiCH_2NC gave the complex $[\{Ti(\eta^5\text{-}C_5Me_5)(CH_2Ph)(\kappa^2\text{-}C,N\text{-}PhCH_2C{=}NCH_2SiMe_3)\}_2(\mu\text{-}O)]$ (**6**) in moderate yield (63%), as a single stable product. Compounds **3**−**6** are quite soluble in the usual solvents such as benzene, toluene, hexane, or pentane, but **3**−**5** should be stored at low temperature under inert conditions to prevent their decomposition (**3**, **5**) or evolution (**4**) at room temperature, in both solution and solid state. Their nature could be determined by single-crystal X-ray diffraction analysis.

The solid-state structures of compounds **3** and **6** are depicted in Figures 1 and 2, while the analogous molecular structures of **4** and **5** can be found in the Supporting Information. Selected data of **3**−**6** are listed in Table 1. The O atom in **3** and **5** is located on an inversion center, such that the two halves of the molecular are crystallographically equivalent.

The solid-state structure of these compounds reveals a η^2-RCNR′ group on each metal center in typical four-legged piano-stool environments, connected by a bridging oxygen atom. Complexes **3**−**6** can adopt several configurations that depend on the *syn* or *anti* arrangement of the η^5-C_5Me_5 rings as well as the stereochemistry around each chiral metal atom. Thus, while complexes **3** and **5** adopt an *anti* arrangement, compounds **4** and **6** show a *syn* arrangement in solid state. The

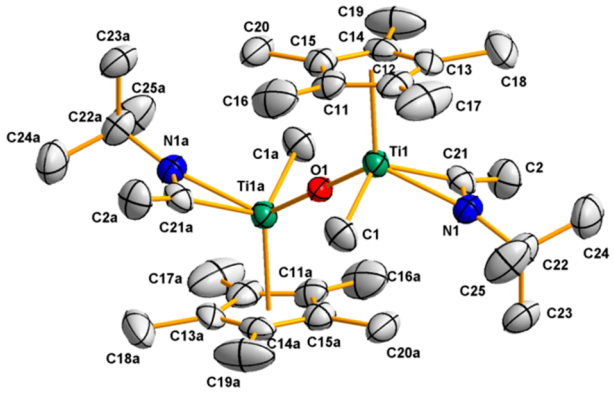

Figure 1. Molecular structure of compound **3**. Thermal ellipsoids are at 50% probability. Hydrogen atoms are omitted for clarity.

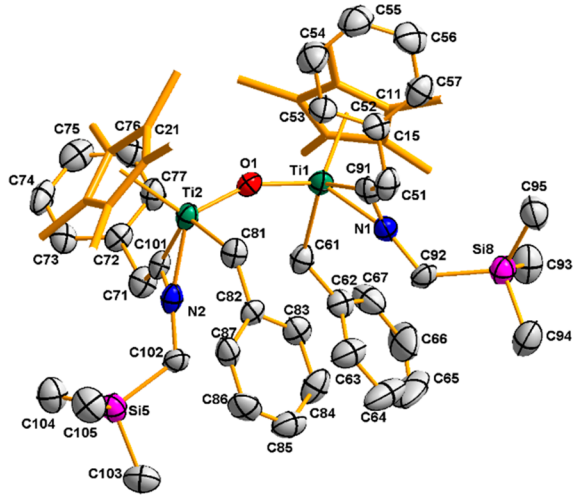

Figure 2. Molecular structure of compound **6**. Thermal ellipsoids are at 50% probability. Hydrogen atoms and carbon atoms of η^5-C_5Me_5 ligands are omitted for clarity.

Table 1. Selected Averaged Lengths (Å) and Angles (deg) for Compounds 3−6

complexes	*anti*-**3**	*syn*-**4**	*anti*-**5**	*syn*-**6**
Ti−O	1.832(1)	1.816(4); 1.823(4)	1.821(1)	1.847(4); 1.838(4)
Ti−N	2.105(4)	2.092(6); 2.075(5)	2.054(3)	2.103(5); 2.083(6)
$Ti-C_{iminoacyl}$	2.049(5)	2.090(7); 2.067(7)	2.076(4)	2.050(7); 2.072(7)
C−N	1.266(6)	1.316(7); 1.276(7)	1.277(5)	1.254(8); 1.263(7)
Ti−O−Ti	180	158.0(2)	166.7(2)	156.4(2)

bond distances Ti−C and Ti−O (see Table 1), although slightly longer than those found in the starting materials **1** (2.11(1) Å, 1.80(1) Å)[27] and **2** (2.133(5)−2.149(5) Å, 1.818(1) Å),[28] are in the expected range for $Ti^{IV}-C(sp^3)$[29,30] and Ti−O[29] bond lengths in other similar oxotitanium species. The existence of the η^2-iminoacyl ligand barely changes the Ti−O−Ti angle in compounds **4** and **6**, while these values in complexes **3** and **5** are wider than in the precursor complex **1** (153.4(1)°).[27] Geometrical parameters for the Ti-η^2-iminoacil bonding system are in the range found for monocyclopentadienyl titanium complexes.[1,31−34]

https://doi.org/10.1021/acs.organomet.1c00300
Organometallics 2021, 40, 2610−2623

The ^{1}H NMR spectrum of freshly obtained crystals of **3**−**5** in benzene-d_6 revealed the existence of isomers with a molar ratio of ≈1:5 for compounds **3** and **5** (see the Experimental Section) and, in the case of complex **4**, the evolution compound **7** (Scheme 3). Thus, the ^{1}H NMR data reveal for

Scheme 3. Spontaneous Rearrangement of 4 to 7

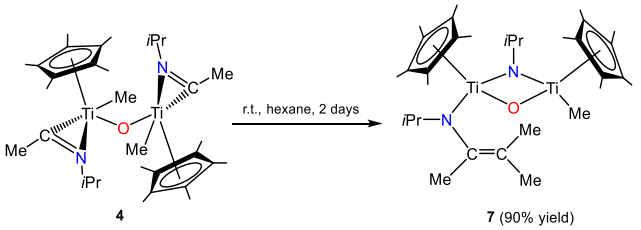

the major isomer of complexes **3** and **5** and for complex **4** one signal for the C_5Me_5 rings, indicative of the same electronic environment around the titanium atoms, one resonance for the methyl groups bonded to titanium and another for the methyl of the η^2-iminoacyl moieties. In addition, the spectra reveal the characteristic signals assigned to the alkyl substituents R′N═CR (R′ = *t*Bu, *i*Pr, CH_2SiMe_3) (see the Experimental Section for the minor isomer). The existence of the η^2-iminoacyl ligand is confirmed in the IR spectra by a stretching band for the C═N bond in the range 1594−1637 cm^{-1}.[1−3,31−34]

As mentioned above, compounds **3** and **5** are unstable and rapidly decompose at room temperature to an unidentifiable mixture of products. In contrast, complex **4** is an unstable substance that steadily evolves in solution at room temperature, and after a few days, complex **7** is entirely obtained in a spectroscopically pure form (see Scheme 3). The preparative-scale synthesis was carried out in hexane to give compound **7** as a dark red crystalline solid in good yield (90%).

Distinguishing features of the ^{1}H NMR spectrum of **7** are two well-separated C_5Me_5 signals indicative of different electronic environments around the titanium centers. In addition, a resonance at 0.79 ppm is consistent with a methyl ligand bound to titanium.[26,27] On the other hand, the migrated methyl groups appear in the range 1.59−1.80 ppm, in agreement with the data reported for the mononuclear alkenylamido tantalum derivative [Ta(η^5-C_5Me_5)Me(NR)-(NRCMe═CMe_2)] (R = 2,6-$Me_2C_6H_3$).[15] These latter signals appear in the ^{13}C{^{1}H} NMR spectrum at a higher field (20.3−26.9 ppm) than that corresponding to the methyl group bound to titanium (38.0 ppm). Furthermore, the signals at 118.6 [C(Me)═CMe_2] and 141.5 [*C*(Me)═CMe_2] ppm are assignable to the alkenyl carbon atoms. Additional evidence for a C═C double bond in **7** is a stretch band at 1644 cm^{-1} in the infrared spectrum. The resulting evolution of **4** diverges from that observed for group 4 complexes in which the coupling of the two η^2-iminoacyl groups undergoes net rearrangement to afford a metal-bound enediamido moiety (see Scheme 1B).[5,13] In contrast, the analysis of the NMR data of the isolated product **7** seems to indicate that both iminoacyl groups in **4** have transformed into bridging imido and terminal alkenylamido fragments. The formation of the imido/vinylamido functions has precedent in mononuclear species, especially with early transition metals.[35−43]

In view of the results achieved with the alkyl isonitriles, we decided to extend the reactivity study of complexes **1** and **2** with the aromatic isonitrile, XylNC. Thus, while the reaction with complex **1** gave a mixture of unidentified products, the heating of **2** at 65 °C for 4 days with 2 equiv of XylNC let us isolate only complex [{Ti(η^5-C_5Me_5)(CH═CHPh)}(μ-O)-{Ti(η^5-C_5Me_5)(μ-κ^2-N,C—N(MeC_6H_3)CH_2)}] (**8**) (Scheme 4), as determined later by X-ray diffraction analysis.

Scheme 4. Formation of Complex 8

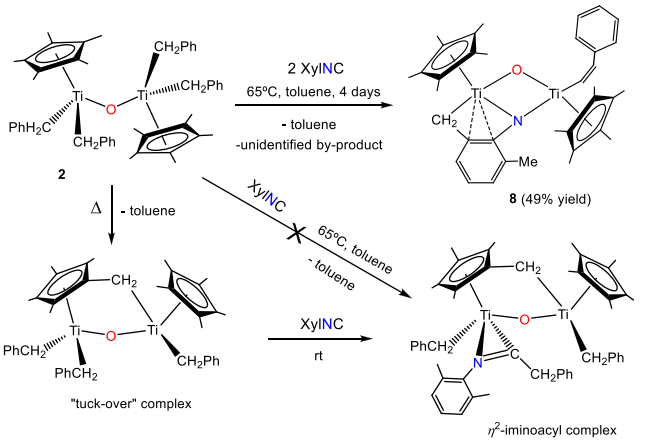

Monitoring the reaction by ^{1}H NMR spectroscopy at room temperature in a 1:1 ratio disclosed the gradual liberation of toluene and the formation of complex **8**, but the addition of a second equiv of isonitrile and heating at 65 °C for 4 days is required to achieve a complete transformation. Signals in the ^{1}H NMR spectrum of the final reaction mixture, other than those assignable to complex **8**, could be attributable to thermal decomposition of **8** after being heated at 65 °C for 4 days and/or some organic byproducts; unfortunately we could not identify them. On the other hand, complex **8** is stable both in solution and in solid state at room temperature for long periods of time. Curiously, the formation of a η^2-iminoacyl complex, analogous to compounds **3**−**6**, was not detected. It is noteworthy that, despite having all of the necessary reagents and similar experimental conditions to those used to obtain the "*tuck over*" complex [Ti_2(η^5-C_5Me_5)(μ-η^5-$C_5Me_4CH_2$−κC)(CH_2Ph)$_3$(μ-O)][28] and its η^2-iminoacyl derivative,[44] none of them were detected (Scheme 4).

The ^{1}H NMR spectrum of **8** in benzene-d_6 shows two resonances for the C_5Me_5 rings, indicative of different electronic environments around the titanium atoms. The (2-methylene-6-methylphenyl)imido fragment exhibits a single signal at 2.27 ppm for the methyl group and an AX spin system (δ 3.05, 2.01) for the methylene CH_2 group of the xylyl ligand. Typical signals for the alkenyl moiety in the ^{1}H NMR (δ 7.68, 7.69, J = 14.0 Hz), ^{13}C{^{1}H} NMR (δ 190.3, 140.7), and IR spectra (C═C: $\bar{\nu}$ = 1651 cm^{-1}) are found.

The molecular structure of complex **8** is shown in Figure 3. Aside from the two titanium atoms joined by an oxygen atom, this species does not show any structural analogy to compounds **3**−**6**. The Ti1 atom adopts a three-legged piano-stool geometry comprising the centroid of the pentamethylcyclopentadienyl ring, an oxygen, a μ-imido moiety, and a styryl ligand. An analogous environment could be assigned to Ti2 with the η^5-C_5Me_5 ring, O1, N1, and a methylene group, locating the two carbon atoms, C31 and C36, at 2.431(4) and 2.464(4) Å from Ti2, respectively. The bond distances Ti2−C38 (2.123(4) Å) and Ti1−C41 (2.144(4) Å) are in the range found for single Ti−C bonds.[29,30]

https://doi.org/10.1021/acs.organomet.1c00300
Organometallics 2021, 40, 2610−2623

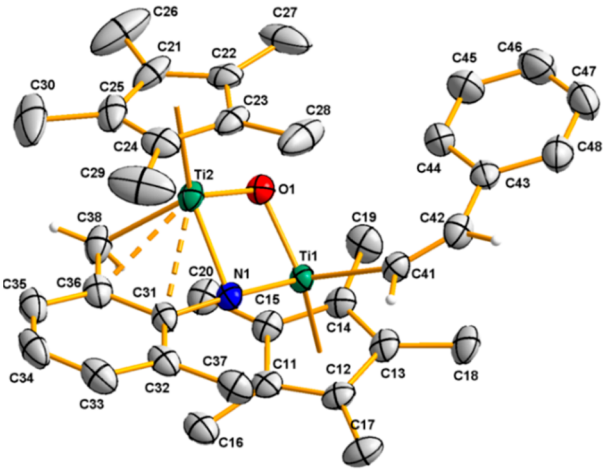

Figure 3. Molecular structure of compound **8**. Thermal ellipsoids are at 50% probability. Most hydrogen atoms are omitted for clarity.

On the other hand, though all Ti−O and Ti−N lengths compare well with a single bond, the coordination of the (2-methylene-6-methylphenyl)imido moiety to both titanium atoms discloses an asymmetry in the central ring; the Ti1−O1 (1.833(2) Å) and Ti1−N1 (1.862(3) Å) bond distances are shorter than Ti2−O1 (1.852(2) Å) and Ti2−N1 (1.988(3) Å). This latter value together with the C31−N1 (1.389(4) Å), C31−C36 (1.430(5) Å), and C36−C38 (1.454(6) Å) bond lengths, between a double and single bond,[45] do not let us to discard π-electronic delocalization along this moiety. The coordination of the (2-methylene-6-methylphenyl)imido moiety through the nitrogen atom and the methylene group makes the Ti1−O1−Ti2 (96.1(1)°) angle clearly narrower than that found for the starting compound **2** (159.1(3)°).[28] Additionally, the bond distance C41−C42 1.324(5) Å, where the metal center and the aromatic ligands adopt a *cis* configuration, is coherent with a double bond.

Reactions with Organic Nitriles. The reactions of complexes $[\{Ti(\eta^5\text{-}C_5Me_5)R_2\}_2(\mu\text{-}O)]$ (R = Me **1**, CH_2Ph **2**) with some nitriles are summarized in Schemes 5−7. The

Scheme 5. Reactions of Complexes 1 with Nitriles

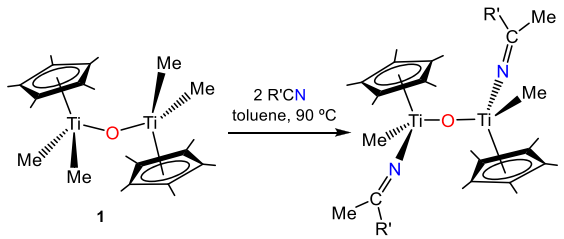

R' = *t*Bu **9** (63% yield), *i*Pr **10** (77% yield)

addition of R′CN (R′ = *t*Bu, *i*Pr) at room temperature to a toluene solution of **1** in a 1:2 molar ratio or an excess, and heating at 90 °C for several days, enabled the selective incorporation of one molecule of nitrile in each titanium center, and complexes **9** and **10** were isolated as orange microcrystalline solids in moderate yields. The NMR spectra showed the presence of isomers, and subsequent heating of the sample gave no evidence of interconversion or a significant change in the ratio. Compound **9** was shown to be *anti*-$[\{Ti(\eta^5\text{-}C_5Me_5)Me(NC(Me)tBu)\}_2(\mu\text{-}O)]$ once X-ray diffraction studies were performed on single crystals obtained from a saturated solution in hexane. The molecular structure is shown in Figure 4 and is discussed below.

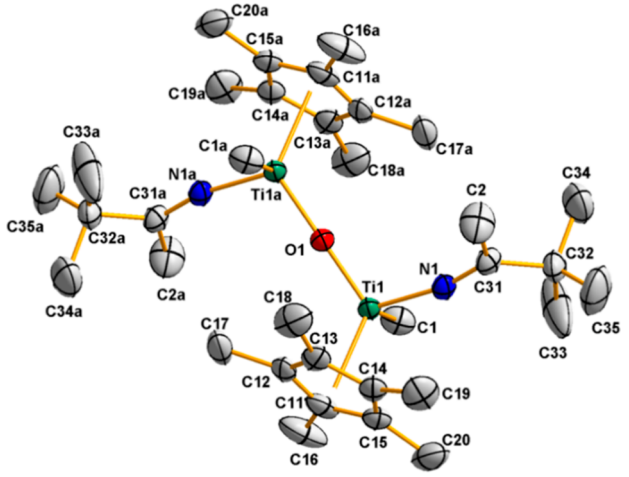

Figure 4. Molecular structure of compound **9**. Thermal ellipsoids are at 50% probability. Hydrogen atoms are omitted for clarity. Selected bond lengths (Å) and angles (deg): Ti1−O1 1.817(1), C31−C32 1.534(4), Ti1−C1 2.135(3); O1−Ti1−N1 108.8(1), N1−C31−C2 120.1(3), O1−Ti1−C1 100.2(1), N1−C31−C32 122.4(2), N1−Ti1−C1 100.2(1), C2−C31−C32 117.5(2).

The ^{1}H and ^{13}C{^{1}H} NMR spectra of freshly obtained crystals of **9** and **10** are consistent with those of symmetrical structures, with an inversion center on the bridging oxygen. These complexes exist as a mixture of isomers as revealed by the doubling of all of the signals in the ^{1}H and ^{13}C NMR spectra of these solutions (see the Experimental Section for the minor isomers). Thus, the spectra show for the major isomer the equivalence of the η^5-C_5Me_5 ligands, with only one signal in the ^{1}H NMR spectra [δ = 1.96 (**9**), 1.98 (**10**)] and two in the ^{13}C{^{1}H} NMR spectra [δ = 12.0 (**9**), 12.0 (**10**) $C_5\mathit{Me}_5$; 119.1 (**9**), 119.1 (**10**) C_5Me_5). Distinguishing features of **9** and **10** are the resonances for the ketimido ligands at δ 1.90/25.1 (**9**) and 1.83/27.3 (**10**) for the methyl group (N=C*Me*R) in the ^{1}H/^{13}C{^{1}H} NMR spectra, and at 183.0 (**9**) and 180.9 (**10**) in the ^{13}C{^{1}H} NMR for the carbon atoms (N=*C*MeR), which evidence the incorporation of the organic nitrile. These values are within the range known for group 4 metal−ketimido complexes.[46−48]

As can be seen in Figure 4, the molecular structure of complex **9** comprises a dinuclear species where each of the titanium atoms adopts a three-legged piano stool arrangement with a ketimido fragment, a methyl group, and an oxygen atom occupying the basal positions and the C_5Me_5 ring in the apical vertex. It is noteworthy that the incorporation of the organic nitrile opens the Ti−O−Ti angle (180.0°) with respect to the precursor complex **1** (153.4(1)°).[27] Structural parameters related to the ketimido fragment, Ti1−N1 1.865(2) Å, N1−C31 1.257(3) Å, and Ti1−N1−C31 167.5(2)°, are similar to those of other titanium(IV)−ketimido complexes.[49−52]

In an attempt to generalize the preparation of **9** and **10**, we treated complex **2** with *t*BuCN and *i*PrCN. To our surprise, the reaction occurs upon heating at 65 °C in a 1:2 molar ratio of the reagents to give the alkenylimido complexes **11** and **12** rather than the expected ketimido species. Moreover, the incorporation of the nitrile only takes place on one of the

https://doi.org/10.1021/acs.organomet.1c00300
Organometallics 2021, 40, 2610−2623

titanium centers (see Scheme 6). By ^{1}H NMR monitoring in benzene-d_6, we observed the slow formation of **11** and

Scheme 6. Reactions of Complexes 2 with Nitriles

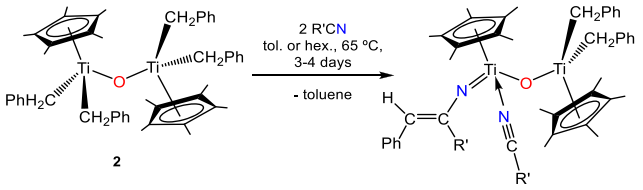

elimination of toluene. Complex **11** was fully characterized by NMR and IR spectroscopy, elemental analysis, and single-crystal X-ray diffraction, while complex **12** could only be characterized by a single-crystal X-ray diffraction study and IR spectroscopy. Compound **12** shows thermal instability in solution (degradation is observed after a few minutes at room temperature) leading to an intractable mixture of products, and therefore, they must be stored in solid state at temperatures below −20 °C.

The solid-state structure of compound **11** is depicted in Figure 5, while the analogous molecular structure of **12**,

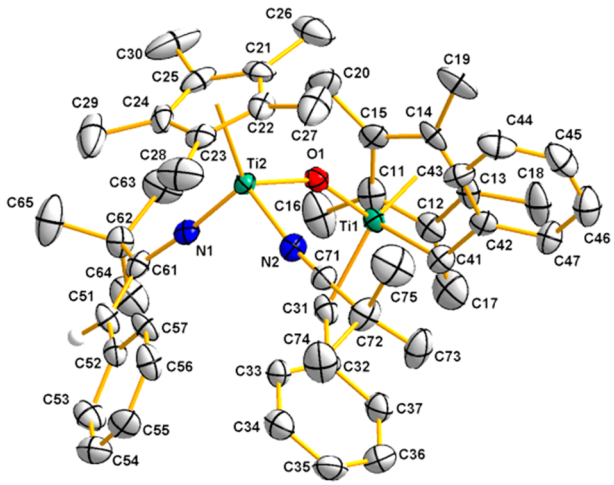

Figure 5. Molecular structure of compound **11**. Thermal ellipsoids are at 50% probability. Hydrogen atoms are omitted for clarity, except that of the alkenyl fragment.

together with the listing of the core bond angles and distances, can be found in the Supporting Information (see Figure S2 and Table S3). Molecular structures of **11** and **12** comprise two Ti(η^5-C_5Me_5)L_2 units bridged by an oxygen atom. Both metal centers exhibit a pseudotetrahedral environment, showing Ti2 in its coordination sphere, an alkenylimido fragment, and a nitrile ligand, while Ti1 remains with two unaltered benzyl groups. In this latter case, the Ti−C bond distances show values (2.126(5)−2.163(5) Å) quite similar to those found in complex **2** (2.133(5)−2.149(5) Å),[28] coherent with no participation of Ti1 in the reaction.

The coordination of the nitrile ligand and the alkenylimido fragment to Ti2 increases the electronic density on the metal center and elongates the distance Ti2—O1 (1.899(3) Å) with respect to Ti1—O1 (1.779(3) Å). Additionally, the Ti—O—Ti bond angle (149.2(2)°) is approximately 10° narrower than that of the precursor **2** (Ti1—O1—Ti1a = 159.1(3)°), probably due to the existence of C—H···π stacking interactions in these compounds (for more details, see Figure S3 and Table S4 in the Supporting Information). The nature of the titanium imido interaction is confirmed by the Ti2—N1 (1.747(4) Å **11**, 1.744(3) Å **12**) and N1—C61 (1.372(6) Å **11**, 1.374(5) Å **12**) bond distances and the angle Ti2—N1—C61 (174.0(4)° **11**, 172.1(3)° **12**), within the known values for imido-titanium(IV) species.[53−55] Moreover, the bond lengths C51—C61 (1.361(7) Å **11**, 1.356(6) Å **12**) and C51—C52 (1.452(7) Å **11**, 1.460(6) Å **12**) show typical values for C(sp^2)=C(sp^2) or C(sp^2)—C(sp^2) bonds, respectively. Finally, the structural parameters for the nitrile moiety (Ti2—N2 = 2.151(4) **11**, 2.131(3) Å **12**; N2—C71 = 1.139(6) **11**, 1.151(5) Å **12**; Ti2—N2—C71 = 173.2(5)° **11**, 170.1(3)° **12**; N2—C71—C72 = 177.6(6)° **11**, 179.7(5)° **12**) are in the range found for other nitrile titanium complexes[56−58] in which the linearity of the Ti—N≡C fragment is shown.

The ^{1}H and ^{13}C{^{1}H} NMR spectra of **11** confirm that the molecular structure obtained by the X-ray diffraction study is maintained in solution. In this sense, and in an analogous fashion to compound **7**, the NMR spectra show the inequivalence of the η^5-C_5Me_5 ligands, with two signals in the ^{1}H NMR spectra (δ = 1.85, 2.10) and four in the ^{13}C{^{1}H} NMR spectra (δ = 12.2, 11.9, C_5Me_5; 122.1, 120.1 C_5Me_5). Additionally, the ^{1}H NMR spectrum exhibits as more remarkable features a singlet at δ 5.52 for the proton on the alkenyl fragment [TiNC(*t*Bu)=C*H*Ph] and one AX and other AB spin systems for the methylene CH_2 groups of the benzyl ligands. Furthermore, the signals of the ^{13}C{^{1}H} NMR spectrum at 106.2 and 123.9 ppm are assignable to the alkenyl carbon atoms [TiN*C*(*t*Bu)=*C*HPh], and the resonance for the carbon atom of the coordinated N*C*tBu moiety appears at 167.7 ppm. The existence of the nitrile ligand is confirmed by a stretching band for the N≡C bond at 2256 (**11**) and 2266 (**12**) cm^{-1} in the IR spectra.

Finally, Me_3SiCN was used to extend the study on nitrile insertion processes. In this sense, the reactions did not proceed to obtain products of type **9**/**10** or **11**/**12**. Moreover, there was no reaction with **2**, and treatment of complex **1** with Me_3SiCN afforded the azatitanacyclopropane isocyanide complex [{Ti(η^5-C_5Me_5)Me_2}(μ-O){Ti(η^5-C_5Me_5)(κ^2-C,N−Me_2CN$SiMe_3$)(CN$SiMe_3$)}] (**13**), as determined later by an X-ray diffraction analysis (Scheme 7). Complex **13** decomposes in solution, precluding its characterization by ^{13}C{^{1}H} NMR, although the ^{1}H NMR spectrum could be recorded immediately after NMR tube preparation.

Although, since the mid-1970s, it has been known that trialkylsilylnitriles exist in equilibrium with R_3SiNC,[59] examples of the nitrile−isocyanide rearrangement in the presence of an organometallic complex are rare. Thus, Bochmann et al. reported that trimethylsilylnitrile isomerizes to the isocyanide

Scheme 7. Reactions of Complexes 1 with Me_3SiCN

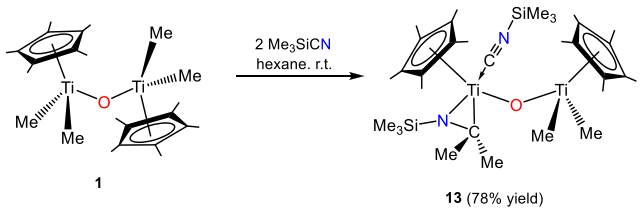

https://doi.org/10.1021/acs.organomet.1c00300
Organometallics 2021, 40, 2610−2623

and forms the η^2-iminoacyl complex [$Cp_2Ti(Me_3SiN{=}CMe)(C{\equiv}NSiMe_3)$]$BPh_4$, possibly due to the fact that, in these systems, the formation of titanium—carbon bonds is favored with respect to titanium—nitrogen bonds.[47] Furthermore, the double migratory insertions of two methyl groups to a coordinated isocyanide to give an azametallacyclopropane species are known for a few examples with early transition metals.[60−65]

To confirm unambiguously the structural connectivity in this species, quality crystals suitable for an X-ray study were obtained. The solid-state structure of **13** is shown in Figure 6.

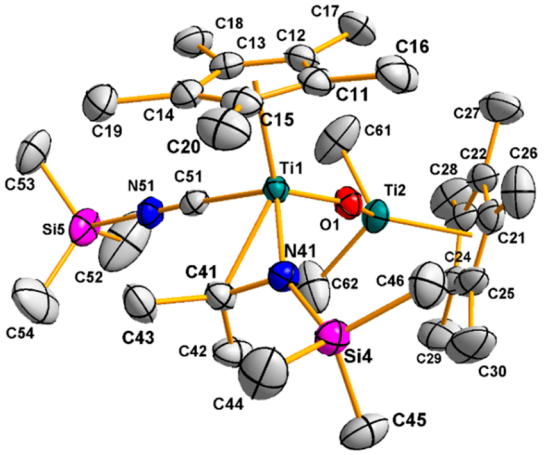

Figure 6. Molecular structure of compound **13**. Thermal ellipsoids are at 50% probability. Hydrogen atoms are omitted for clarity.

It consists of a dinuclear species where each metal center exhibits different coordination environments. The five-coordinated titanium atom, Ti1, adopts a four-legged piano-stool geometry with a (κ^2-C,N−$Me_2CNSiMe_3$) fragment, a trimethylsilyl isocyanide group, and an oxygen atom occupying the basal positions while the C_5Me_5 ring again is located at the apical vertex. The Ti2 center shows a pseudotetrahedral environment with a C_5Me_5 ligand, two methyl groups, and an oxygen atom, with no significant structural differences with respect to the starting material **1**. The Ti1−O−Ti2 angle (153.7(1)°) is nearly identical to that observed in precursor complex **1** (153.4(1)°),[27] even with the major steric hindrance around Ti1. As expected, the different electronic environment around each metal center produces notable structural differences. For example, Ti1−O1 (1.862(2) Å) is clearly longer than Ti2−O1 (1.786(2) Å), according to the higher electronic deficiency on Ti2, and these are comparable values to those observed in other dinuclear oxotitanium asymmetric species.[44,66] The trimethylsilyl-isocyanide is end-on bonded and nearly linear (Ti1−C51−N51 175.0(3)°), with Ti1−C51 of 2.092(3) Å and a short bond distance N51−C51 of 1.160(4) Å typical of the carbon−nitrogen triple bond, comparable to those found in coordinated isocyanide Ti(IV) complexes.[67−70] The azatitana-cyclopropane moiety in **13** shows typical single bond distances Ti1−N41 (1.956(2) Å), Ti1−C41 (2.185(3) Å), and C41−N41 (1.408(4) Å),[29] similar to the values found for the few examples of titanaaziridine derivatives[71−75] and for other early transition metals, especially tantalum.[13,76,77]

The ^{1}H NMR spectrum of **13** in benzene-d_6 shows two resonances for the C_5Me_5 rings, indicative of different electronic environments around the titanium atoms. Analogously, this spectrum reveals two resonances for the methyl groups bound to titanium (0.30 and 0.29 ppm), two signals for the methyl groups of the azatitanacyclopropane unit at δ 1.32 and 1.85, and one signal (0.52 ppm) for the methyl groups of the $SiMe_3$ fragment, in accord with the asymmetry of **13**. Moreover, the existence of the isocyanide ligand is confirmed by a stretching band for the C≡N bond at 2036 cm^{-1} in the IR spectrum, comparable to those found in Ti(IV) complexes with coordinated isocyanides.[67,78−81]

Computational Studies. In order to clarify the mechanism of some of the reactions experimentally observed and to understand the diversity of products observed as a function of the nitriles or isonitriles employed in the reactions, selected transformations were also studied by DFT calculations at the PBE0-D3(BJ)/Def2-TZVP//PBE0-D3(BJ)/Def2-SV(P) level of theory.[82−89]

The migratory insertion processes to yield the previously described η^2-iminoacyl complexes **3**−**6**, as a result of the participation of the two metal centers, were fully analyzed first using the complex [{Ti(η^5-C_5Me_5)Me_2}$_2$(μ-O)] (**1**) and the simplest R′NC isonitrile (R′ = Me) as a model. Then, several calculations were also carried out with a bulkier isonitrile (R′ = *t*Bu) to test the influence of the R′ group on the isomers obtained and in the subsequent reactivity of the η^2-iminoacyl complexes. Finally, selected calculations were also performed for the analogous reactions with the complex [{Ti(η^5-C_5Me_5)$(CH_2Ph)_2$}$_2$(μ-O)] (**2**). The thermodynamic and kinetic parameters computed for the well-known isonitrile insertion into the Ti-alkyl bonds of complex **1** to form the corresponding η^2-iminoacyl complexes are collected in Scheme 8 (for a graphical representation of the whole mechanism, see Figure S4 in the Supporting Information).[1−4]

Scheme 8. Computed ΔG(25 °C) Values for the R′NC Insertion Reactions on Complex 1 (R′ = Me, ^{t}Bu)[a]

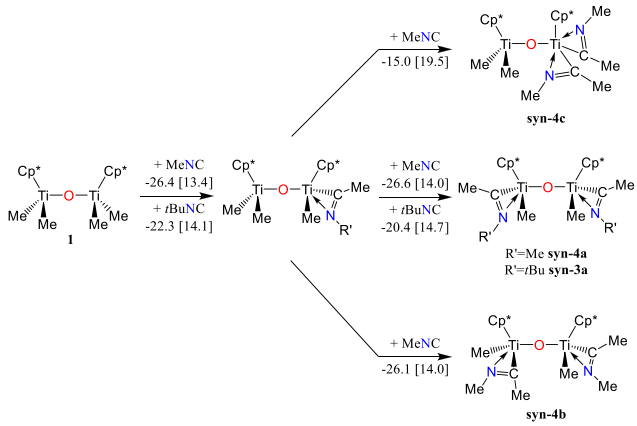

[a]Between brackets, $\Delta G^{\ddagger}$(25 °C) values. All data in kcal mol^{-1}. Cp* = (η^5-C_5Me_5).

As can be seen in Scheme 8, all insertion processes studied are thermodynamically favorable and present easily affordable barriers at room temperature or below in agreement with experimental findings. Once the first insertion has occurred, the second isocyanide could be inserted on any of the remaining Ti−Me bonds leading to three different isomers (**4a**−**4c**) as shown in Scheme 8, being thermodynamically and kinetically more favorable when it takes place on the second metallic center, bounded to two alkyl groups leading to compounds **4a** or **4b**. In this regard, there are no significant

https://doi.org/10.1021/acs.organomet.1c00300
Organometallics 2021, 40, 2610−2623

differences in the ΔG(25 °C) or $\Delta G^{\ddagger}$(25 °C) values computed for the first and the second MeNC insertion processes when the second occurs in the titanium center containing two uninserted alkyl moieties to give either complexes **4a** or **4b**. All insertion processes shown in Scheme 8 are irreversible at 25 °C since the activation barriers for the reverse reactions are in the range 35−40 kcal mol^{-1}. Based on the irreversibility of the insertion processes at 25 °C and the minor differences computed for the activation Gibbs energy for the formation of the two more kinetically favorable species *syn*-**4a** and *syn*-**4b** ($\Delta\Delta G^{\ddagger}$(25 °C) = 0.5 kcal mol^{-1}, see Figure S4), the concomitant formation of isomer **4b** together with **4a**, the latter with a molecular disposition equivalent to the solid-state structure of **4** (see Figure S1 in the Supporting Information), should also be expected. Likewise, the kinetic barriers computed for the ^{t}BuNC insertions are essentially identical to those previously described for the reactions with the less sterically hindered MeNC isonitrile indicating an insignificant effect on the reaction rate as a function of the steric hindrance of the isonitrile. However, the activation Gibbs energy calculated for the first MeNC addition to complex **2** ($\Delta G^{\ddagger}$(25 °C) = 15.8 kcal mol^{-1}) is 2.4 kcal mol^{-1} higher than that computed for the same reaction with complex **1** in agreement with the observation that the reaction time needed to quantitatively obtain the η^2-iminoacyl complex **6** (hours) is larger than that required to yield compound **5** (minutes) after the insertion of Me_3SiCH_2NC to either complexes **2** or **1**, respectively (see Scheme 2).

Moreover, as stated above, *anti* (**3** and **5**) or *syn* (**4** and **6**) arrangements were observed in the crystalline structures of the iminoacyl complexes, taking into consideration the relative disposition of the pentamethylcyclopentadienyl ligands. Accordingly, the possible interconversion between the *anti* or *syn* conformations was analyzed computationally for **4a** and **4b** species as shown schematically in Scheme 9.

Scheme 9. Computed ΔG(25 °C) Values for the *syn*−*anti* Isomerization Reactions for Compounds 3a, 4a, and 4b[a]

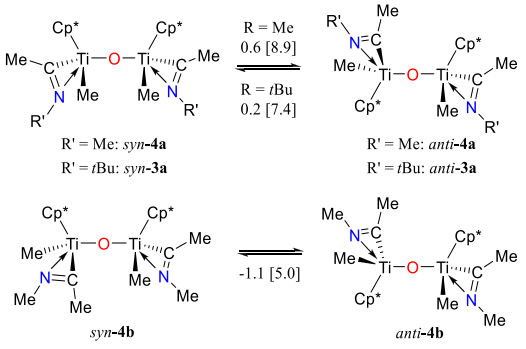

[a]Between brackets, $\Delta G^{\ddagger}$(25 °C) values. All data in kcal mol^{-1}.

The rotations around the oxo bridge interconverting *syn* and *anti* conformers are again easily affordable processes in mild conditions, as can be inferred by the thermodynamic and kinetic values computed and reported in Scheme 9. In this sense, the almost identical Gibbs energy values for the *syn* and *anti* conformers of both **4a** and **4b** diastereomers and the low activation Gibbs energy values computed for that interconversion support a dynamic equilibrium between *syn* and *anti* conformers occurring faster than the NMR time scale. Similarly, the interconversion between *syn*-**3a** and *anti*-**3a** (R′ = *t*Bu) was also computed (see Scheme 9), and the results are quite similar to those observed for the rotation around the oxo bridge in compound **4a**. Consequently, only one resonance attributable to both species (*syn* and *anti* of each isomer **3a**, **4a**, or **4b**) should be expected in the NMR spectra at room temperature in solution. However, the interconversion between diastereomers **4a** and **4b** requires the elimination of one isonitrile already inserted and a subsequent insertion in the other Ti−Me bond of the same titanium center. Nevertheless, as stated previously, all isonitrile insertions shown in Scheme 8 are irreversible under mild conditions, and thus, we can reject the possibility of interconversion between different diastereomers such as **4a** and **4b** at room temperature or below.

In addition to the plausible formation of the isomers analyzed in Schemes 8 and 9, the rotation of the iminoacyl ligands lead to different isomers (*endo*−*exo*) as described in Scheme 10 for compounds *anti*-**4a** (R′ = Me) and *anti*-**3a** (R′ = *t*Bu) and as previously reported for other η^2-iminoacyl complexes.[1,90−93]

Scheme 10. Computed ΔG(25 °C) Values for the *endo*−*exo* Isomerization Reactions for Compounds 3a and 4a[a]

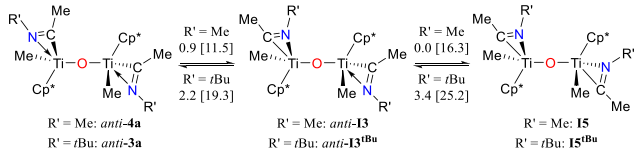

[a]Between brackets, $\Delta G^{\ddagger}$(25 °C) values. All data in kcal mol^{-1}.

The computed Gibbs energy differences among the three isomers of the less sterically crowded complex *anti*-**4a** shown in Scheme 10 are lower than 1 kcal mol^{-1} in line with the possibility of their existence in equilibrium under experimental conditions. Furthermore, the data also indicate a facile rotation of both η^2-iminoacyl ligands for *anti*-**4a** (R′ = Me), although the activation barrier for the first *endo*−*exo* isomerization (*anti*-**4a** → *anti*-**I3**) is about 5 kcal mol^{-1} lower than the corresponding one for the second one (*anti*-**I3** → **I5**). An alternative scenario with *endo*−*exo* isomerizations occurring in complex *syn*-**4a** and then a rotation to achieve the corresponding *syn*−*anti* isomerization to finally yield compound **I5** was also explored *in silico* leading to similar results as shown in Figure S5 in the Supporting Information. In the case of the more sterically hindered iminoacyl complexes with a bulkier substituent in the nitrogens such as that in *anti*-**3a** (R′ = *t*Bu), larger thermodynamic differences are observed among the three different isomers as shown in Scheme 10. Moreover, the isomerization processes for *anti*-**3a** exhibit high kinetic barriers, and the formation of *anti*-**I3**$^{t\mathrm{Bu}}$ and its conversion to **I5**$^{t\mathrm{Bu}}$ would be too slow to occur under the experimental conditions.

Thus, according to the values in Schemes 8−10, several isomers are accessible, and some of them can coexist in equilibrium as was also experimentally observed. Although this DFT study has been performed mainly using [{Ti(η^5-C_5Me_5)Me_2}$_2$(μ-O)] (**1**) and MeNC as models, the data obtained from calculations show a good agreement with the experimental results as revealed by the crystalline structures determined for complexes **3**−**6**, with the same arrangement as the computed species *syn*-**4a** (complex **4**, see Figure S1), *anti*-

https://doi.org/10.1021/acs.organomet.1c00300
Organometallics 2021, 40, 2610−2623

4a (complex **3**, see Figure 1), *syn*-**4b** (complex **6**, see Figure 2), and *anti*-**4b** (complex **5**, see Figure S1).

Once the insertion processes have been analyzed, it would be interesting to know how the formation of the imido-vinylamido complex $[Ti_2(\eta^5\text{-}C_5Me_5)_2(\mu\text{-}O)(\mu\text{-}NiPr)\{N(iPr)\text{-}CMe{=}CMe_2\}Me]$ (**7**) by rearrangement of **4** takes place. Given the reliability of the calculations performed with the methyl substituted models, we decided to study the evolution of complex *syn*-**4a**. In that sense, Schemes 9 and 10 show the required isomerizations (*syn* → *anti* and *endo* → *exo*) to form intermediate **I5** from *syn*-**4a**, with easily affordable barriers at room temperature for this slightly endergonic transformation (ΔG(25 °C) = 1.6 kcal mol^{-1}). As mentioned above, an alternative possibility with *endo* → *exo* isomerizations occurring before the *syn* → *anti* isomerization was also computed, and the results obtained (see Figure S5 in the Supporting Information) are similar to those presented in Schemes 9 and 10. A plausible mechanistic scenario for the reaction yielding the final imido-vinylamido product **7a** is collected in Figure 7 starting from the bis(*anti*-η^2-iminoacyl)

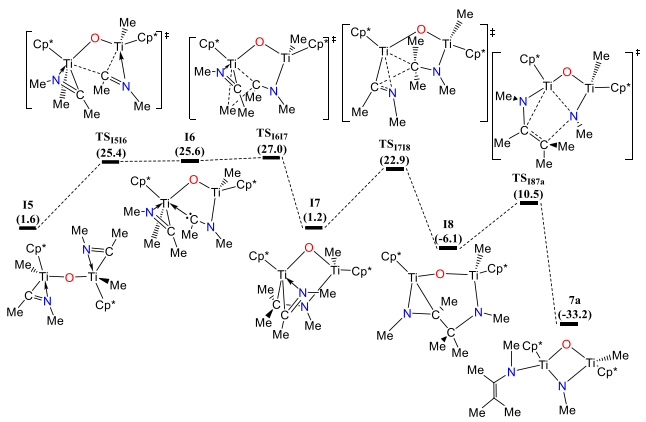

Figure 7. Gibbs energy profile at 25 °C (kcal mol^{-1}) in the formation of **7a**.[94]

intermediate **I5** located at 1.6 kcal mol^{-1} related to the starting reactant *syn*-**4a** (0.0 kcal mol^{-1}). The presence of two adjacent metallic centers favors that one of the two iminoacyl groups in **I5** could be converted into an amidocarbene bridging fragment in **I6**. The proximity of this group to a Ti—Me bond gives rise to a second insertion process to obtain intermediate **I7**. The migration of the CMe_2NMe moiety to the η^2-iminoacyl group renders the last intermediate **I8** that easily evolves by a surprising C—N cleavage step to the imido-vinylamido compound **7a**. The activation Gibbs energy for the rearrangement of the bis(η^2-iminoacyl) complex **I5** to yield **7a** is associated with the formation of the high-energy species carbene **I6** and the following insertion into the Ti—Me bond overcoming $\mathbf{TS_{I6I7}}$. The Gibbs energy barrier computed for this transformation (27 kcal/mol) is in agreement with the rearrangement of complex **4** to yield species **7** (see Scheme 3) occurring in several days at room temperature. However, the formation of the required $\mathbf{I5^{tBu}}$ intermediate from the most stable isomer *syn*-**3a** (R′ = *t*Bu) is 5.7 kcal mol^{-1} uphill what would increase the kinetic barrier for an analogous rearrangement when R′ = *t*Bu, and this could be the reason why this reaction was not observed experimentally for η^2-iminoacyl complexes with the bulkier substituents and why it has only been observed in the case of **4** containing the less sterically hindered R′NC.

An alternative mechanism for the formation of **7a** from **4a** through the plausible coupling between iminoacyl groups to form an enediamido species (see Scheme 1B) was also explored, but the higher Gibbs activation energy computed ($\Delta G^{\ddagger}$(25 °C) = 42.4 kcal mol^{-1}) leads to the rejection of this path. For more details, see Figure S6 in the Supporting Information.

Finally, we focus our attention on the formation of the unexpected alkenyl imido derivatives **11** and **12**. Following the procedure carried out for the isonitrile reactions, we performed DFT calculations using complex $[\{Ti(\eta^5\text{-}C_5Me_5)\text{-}(CH_2Ph)_2\}_2(\mu\text{-}O)]$ (**2**) and MeCN as a model to simplify the study. A schematic Gibbs energy diagram computed for this process is shown in Figure 8. The first transformation

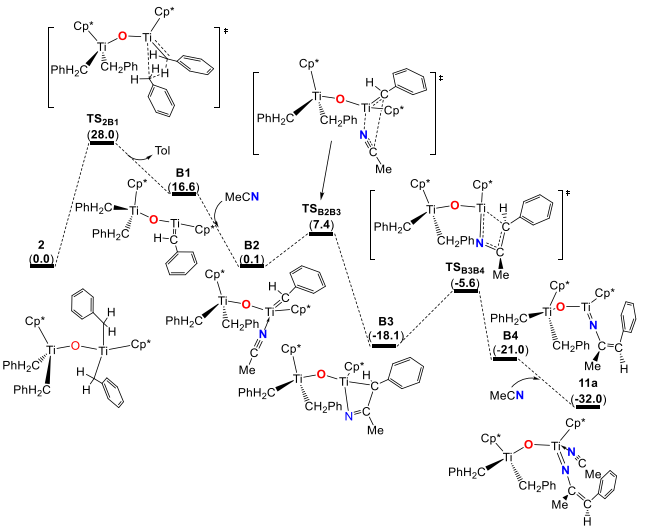

Figure 8. Gibbs energy profile at 25 °C (kcal mol^{-1}) for the reaction of MeCN with complex **2**.

consists of an α-H abstraction, and it is the rate-determining step of the whole process studied with a high kinetic barrier ($\Delta G^{\ddagger}$(25 °C) = 28.0 kcal mol^{-1}) consistent with the experimental reaction conditions (see Scheme 6 and the Experimental Section). The formation of alkylidene intermediate **B1** has been previously proposed in the thermal treatment of complex **2** that, in the absence of other additional ligands, produces the "tuck over" complex shown in Scheme 4.[28] However, in the presence of nitrile ligands as in the reaction conditions where compounds **11** and **12** were obtained, the nitrile coordinates to the alkylidene intermediate **B1** in a barrierless process, yielding the intermediate **B2**. Then, an intramolecular [2 + 2] addition between the MeCN and the alkylidene ligands[93] ($\mathbf{TS_{B2B3}}$) is easily produced to give the intermediate **B3**. After that, an electronic redistribution within the azatitanacyclobutene through $\mathbf{TS_{B3B4}}$ renders the alkenyl imido **B4**. Finally, a second MeCN molecule fills the titanium coordination sphere to yield **11a**, as a model of complexes **11** and **12**. Although this study has been carried out using MeNC as a nitrile model, the results are expected to be similar for other nitriles since, as stated before, the rate-determining step is the first dissociative process to form the alkylidene intermediate (**B1**), and the nitrile ligands play a role later in the mechanisms.

https://doi.org/10.1021/acs.organomet.1c00300
Organometallics 2021, 40, 2610−2623

CONCLUSIONS

A new series of dinuclear μ-oxo titanium complexes have been synthesized and characterized as a result of Ti—C insertions, C—N cleavage, or C—C formation reactions with either organic isocyanides or nitriles. The reactivity of the starting complexes $[\{Ti(\eta^5\text{-}C_5Me_5)R_2\}_2(\mu\text{-}O)]$ (R = Me, CH_2Ph) with the isocyanides R′NC (R′ = *t*Bu, *i*Pr, CH_2SiMe_3) afforded the expected η^2-iminoacyl compounds. However, complex $[\{Ti(\eta^5\text{-}C_5Me_5)(i\text{PrNCMe})Me\}_2(\mu\text{-}O)]$ cleanly evolved to give the imido-vinylamido derivative $[Ti_2(\eta^5\text{-}C_5Me_5)_2(\mu\text{-}O)(\mu\text{-}N i\text{Pr})\{N(i\text{Pr})CMe{=}CMe_2\}Me]$. In this case, DFT calculations support the formation of an amidocarbene bridge intermediate and subsequent migration processes to render the imido-vinylamido compound, excluding a traditional direct coupling of two η^2-iminoacyl units. Also, the treatment of $[\{Ti(\eta^5\text{-}C_5Me_5)(CH_2Ph)_2\}_2(\mu\text{-}O)]$ with XylNC results in another example of the rich reactivity of these derivatives. On the other hand, the treatment of $[\{Ti(\eta^5\text{-}C_5Me_5)Me_2\}_2(\mu\text{-}O)]$ with *t*BuCN or *i*PrCN generated species in which one ketimido moiety is linked to each metallic center. In a similar way, the reactions of $[\{Ti(\eta^5\text{-}C_5Me_5)(CH_2Ph)_2\}_2(\mu\text{-}O)]$ with *t*BuCN and *i*PrCN gave alkenylimido derivatives, likely through a transient alkylidene fragment as the directing group for the C—H activation. Finally, the analogous reaction with Me_3SiCN leads to the azatitanacyclopropane isocyanide complex $[\{Ti(\eta^5\text{-}C_5Me_5)Me_2\}(\mu\text{-}O)\{Ti(\eta^5\text{-}C_5Me_5)(\kappa^2\text{-}C,N\text{—}Me_2CNSiMe_3)(CNSiMe_3)\}]$, as result of a preceding nitrile–isonitrile isomerization process in solution.

EXPERIMENTAL SECTION

General Considerations. All manipulations were carried out under a dry argon atmosphere using Schlenk-tube and cannula techniques or in a conventional argon-filled glovebox. Solvents were carefully refluxed over the appropriate drying agents and distilled prior to use: C_6D_6 and hexane (Na/K alloy), tetrahydrofuran (Na/benzophenone), and toluene (Na). Starting materials $[\{Ti(\eta^5\text{-}C_5Me_5)R_2\}_2(\mu\text{-}O)]$ (R = Me **1**, CH_2Ph **2**)[25] were prepared following reported procedures. All of the isonitriles (RCN, R = *i*Pr, *t*Bu, CH_2SiMe_3, Xyl) and nitriles (RCN, R = *i*Pr, *t*Bu, $SiMe_3$) were purchased from Aldrich and were used as received. Microanalyses (C, H, N, S) were performed in a LECO CHNS-932 microanalyzer. Samples for IR spectroscopy were prepared as KBr pellets and recorded on the PerkinElmer IR-FT Frontier spectrophotometer (4000−400 cm^{-1}). ^1H and ^{13}C NMR spectra were obtained by using Varian NMR System spectrometers, Unity-300 Plus, Mercury-VX, and Unity-500, and reported with reference to solvent resonances. $^1H-^{13}C$ gHSQC was recorded using the Unity-500 MHz NMR spectrometer operating at 25 °C.

Caution. Reactions with these nitriles and isonitriles should not be undertaken without proper safety precautions put in place. In particular, Me_3SiCN is extremely toxic (fatal if swallowed, in contact with skin, or inhaled).

Preparation of $[\{Ti(\eta^5\text{-}C_5Me_5)Me(\kappa^2\text{-}C,N\text{—}MeCNtBu)\}_2(\mu\text{-}O)]$ (3). To a solution of **1** (0.200 g, 0.45 mmol) in 10 mL of hexane placed into a 25 mL Schlenk tube, *t*BuNC (0.078 g, 0.92 mmol) was added. The resulting solution was stirred for 1 min and then immediately cooled at −35 °C to give, after a few days, orange crystals (0.255 g, 93%) identified as **3**. The ^1H NMR revealed the presence of a mixture of two isomers in a ca. 1:5 ratio. IR (KBr, cm^{-1}): $\bar{\nu}$ = 2911 (s, CH aliph.), 1637 (s, C═N), 1457, 1365 (m, CC), 1103, 1025 (w, CC), 739 (vs, Ti—O—Ti). ^1H NMR (C_6D_6, 300 MHz, 298 K): major isomer, δ = 0.40 (s, 6H, TiMe), 1.31 (s, 18H, *t*Bu), 1.85 (s, 30H, C_5Me_5), 2.49 (s, 6H, η^2-NCMe); minor isomer, δ = 0.19 (s, 6H, TiMe), 1.32 (s, 18H, *t*Bu), 1.88 (s, 30H, C_5Me_5), 2.55 (s, 6H, η^2-NCMe). Elemental Anal. (%) Calcd for $C_{34}H_{60}N_2OTi_2$ (608.58): C, 67.10; H, 9.94; N, 4.60. Found: C, 67.05; H, 9.00; N, 4.80.

Preparation of $[\{Ti(\eta^5\text{-}C_5Me_5)Me(\kappa^2\text{-}C,N\text{—}MeCNiPr\}_2(\mu\text{-}O)]$ (4). A 0.065 g (0.90 mmol) portion of *i*PrNC was added to a vial containing a solution of **1** (0.200 g, 0.45 mmol) in hexane (∼10 mL). The solution readily changed from yellowish to orange and immediately was cooled to −35 °C to yield, after a few days, orange crystals of **4** (0.175 g, 67% yield). The ^1H NMR revealed the presence of complex **7** in a ca. 1:5 ratio. IR (KBr, cm^{-1}): $\bar{\nu}$ = 2970, 2889 (vs, CH aliph.), 1618 (s, C═N), 1446, 1371 (vs, CC), 1103, 1023 (w, CC) (w), 798 (vs, Ti—O—Ti). ^1H NMR (C_6D_6, 300 MHz, 298 K): δ = 4.06 (hept., J = 6.6 Hz, 2H, $CHMe_2$), 2.21 (s, 6H, NCMe), 1.85 (s, 30H, C_5Me_5), 1.28 (d, J = 6.6 Hz, 6H, $CHMeMe$), 1.10 (d, J = 6.3 Hz, 6H, $CHMeMe$), 0.42 (s, 6H, TiMe). Anal. Calcd for $C_{32}H_{56}N_2OTi_2$ (580.53): C, 66.21; H, 9.72; N, 4.83. Found: C, 65.97; H, 9.07; N, 4.97.

Preparation of $[\{Ti(\eta^5\text{-}C_5Me_5)Me(\kappa^2\text{-}C,N\text{—}MeCN\text{-}CH_2SiMe_3)\}_2(\mu\text{-}O)]$ (5). Complex **1** (0.200 g, 0.45 mmol) was dissolved in hexane (10 mL), and Me_3SiCH_2NC (0.103 g, 0.90 mmol) was added to the yellow solution. The resulting solution was quickly stirred and then was cooled at −35 °C to give a crystalline yellow solid (0.265 g, 88%) identified as **5**. IR (KBr, cm^{-1}): $\bar{\nu}$ = 2856 (m, CH aliph.), 1937 (w, CH aliph.), 1630 (s, C═N), 1443, 1377, 1097, 1027 (m, CC), 765 (vs, Ti—O—Ti). ^1H NMR (C_6D_6, 300 MHz, 298 K): major isomer, δ = 0.02 (s, 18H, CH_2SiMe_3), 0.37 (s, 6H, TiMe), 1.88 (overlapping, s, 30H, C_5Me_5), 2.22 (s, 6H, η^2-NCMe), 3.57, 3.37 (AB syst., J = 12.6 Hz, 4H, CH_2SiMe_3); minor isomer, δ = 0.05 (s, 18H, CH_2SiMe_3), 0.34 (s, 6H, TiMe), 1.88 (overlapping, s, 30H, C_5Me_5), 2.23 (s, 6H, η^2-NCMe), 3.58, 3.38 (AB syst., 4H, CH_2SiMe_3). Elemental Anal. (%) Calcd for $C_{34}H_{64}N_2OSi_2Ti_2$ (668.79): C, 61.06; H, 9.65; N, 4.19. Found: C, 61.03; H, 8.92; N, 4.58.

Preparation of $[\{Ti(\eta^5\text{-}C_5Me_5)CH_2Ph(\kappa^2\text{-}C,N\text{—}PhCH_2CN\text{-}CH_2SiMe_3)\}_2(\mu\text{-}O)]$ (6). To a solution of **2** (0.100 g, 0.13 mmol) in 20 mL of toluene was added Me_3SiCH_2NC (0.031 g, 0.27 mmol). The red solution was left stirring for 2 h at room temperature. After that, the solvent was removed under reduced pressure, and the crude was dissolved in hexane. The red solution was filtered, concentrated to half volume, and cooled to −35 °C to yield reddish orange crystals of **6** (0.085 g, 65%). IR (KBr, cm^{-1}): $\bar{\nu}$ = 2955, 2913 (s, CH aliph.), 2867 (m CH aliph.), 1594 m (C═N), 1483 (s, CC), 1451, 1086 (m, CC), 1026 (s, CC) 837, 807 (s, Ti—O—Ti). ^1H NMR (C_6D_6, 300 MHz, 298 K): δ = −0.01 (s, 18H, CH_2SiMe_3), 1.82 (s, 30H, C_5Me_5), 2.61 (s, 4H, Ti—CH_2Ph), 3.64 (s, 4H, NCCH_2Ph), 4.33, 4.20 (AX syst., ^2J = 16.4 Hz, 4H, CH_2SiMe_3), 6.97−7.50 (m, 20H, Ph). $^{13}C\{^1H\}$ NMR (C_6D_6, 75 MHz, 298 K): δ = −0.49 (CH_2SiMe_3), 12.5 (C_5Me_5), 43.0 (CH_2SiMe_3), 43.0 (NCCH_2Ph), 60.0 (Ti—CH_2Ph), 118.9, 128.8, 127.0, 131.0, 137.6, 154.3 (Ph), 120.7 (C_5Me_5), 233.5 (NCCH_2Ph). Elemental Anal. (%) Calcd for $C_{58}H_{80}N_2OSi_2Ti_2$ (973.17): C, 71.58; H, 8.29; N, 2.88. Found: C, 71.03; H, 8.70; N, 3.61.

Preparation of $[Ti_2(\eta^5\text{-}C_5Me_5)_2(\mu\text{-}O)(\mu\text{-}N i\text{Pr})\{N(i\text{Pr})C(Me){=}CMe_2\}Me]$ (7). In a 50 mL Schlenk tube, **1** (0.200 g, 0.45 mmol) was dissolved in hexane (∼10 mL), and 0.065 g (0.90 mmol) of *i*PrNC was added to the solution. The mixture reaction was left stirring at room temperature, and after 2 days, the red solution was cooled at −35 °C to give dark red crystals of **7** (0.237 g, 90% yield). IR (KBr, cm^{-1}): $\bar{\nu}$ = 2909 (s, CH aliph.), 2575 (w CH aliph.), 1644 (w, C═C), 1491 (d, CC), 1449, 1375 (s, CC), 1127, 1104 (vs, CC), 913, 811 (s, Ti—O—Ti). ^1H NMR (C_6D_6, 300 MHz, 298 K): δ = 5.22, 3.55 (m, ^3J = 6.3 Hz, 2H, NCHMe_2), 2.01, 1.98 (s, 15H, C_5Me_5), 1.59, 1.71, 1.80 (s, 9H, $MeC{=}CMe_2$), 1.36, 1.16, 1.13, 1.09 (d, ^3J = 6.6 Hz, 12H, NCCHMe_2), 0.79 (s, 3H, TiMe). $^{13}C\{^1H\}$ NMR (C_6D_6, 75 MHz, 298 K): δ = 141.5, 118.6 ($MeC{=}CMe_2$), 122.8, 119.2 (C_5Me_5), 61.2, 59.9 (NCHMe_2), 38.0 (TiMe), 29.3, 28.8 (NCHMe_2), 26.9, 22.5, 20.3 ($MeC{=}CMe_2$), 12.3, 12.2 (C_5Me_5). Anal. Calcd for $C_{32}H_{56}N_2OTi_2$ (580.53): C, 66.20; H, 9.72; N, 4.83. Found: C, 66.15; H, 9.11; N, 5.29.

Preparation of $[\{Ti(\eta^5\text{-}C_5Me_5)(HC{=}CH(Ph))\}(\mu\text{-}O)\{Ti(\eta^5\text{-}C_5Me_5)(\mu\text{-}\kappa^2\text{-}N,C\text{—}N(MeC_6H_3)CH_2)\}]$ (8). In a 100 mL J-Young Carious tube, **2** (0.100 g, 0.13 mmol) was dissolved in 20 mL of toluene, and XylNC (0.036 g, 0.27 mmol) was added. The resulting

https://doi.org/10.1021/acs.organomet.1c00300
Organometallics 2021, 40, 2610−2623

red solution was stirred and heated at 65 °C for 4 days. After that, the solution was filtered, and the solvent was removed under vacuum. Then, the crude was dissolved in hexane, and the solution was reduced in volume and cooled to −35 °C to give red single crystals (0.040 g, 49%) of **8**. IR (KBr, cm^{-1}): $\bar{\nu}$ = 2964 (m, CH aliph.), 2906 (vs, CH aliph.), 2858 (s, CH aliph.), 1651 (w, C═C), 1374 (s, CC), 1293, 1257, 1234 (m, CC), 1076, 1022 (w, CC), 775 (vs, Ti—O—Ti). ^{1}H NMR (C_6D_6, 300 MHz, 298 K): δ = 1.55, 1.83 (s, 15H, C_5Me_5), 2.01, 3.05 (AX syst., ^2J = 8.0 Hz, 2H, Ti—$CH_2(C_6H_3)$Me), 2.27 (s, 3H, Ti—$CH_2(C_6H_3)Me$), 7.03−7.90 (m, 8H, Ph), 7.60, 7.68 (dd, ^3J = 14.0 Hz, 2H, Ti—CH═CHPh). ^{13}C{^{1}H} NMR (C_6D_6, 75 MHz, 298 K): δ = 10.9, 11.6 (C_5Me_5), 19.1 (Ti—$CH_2(C_6H_3)Me$), 65.4 (Ti—$CH_2(C_6H_3)$Me), 120.7, 121.0 (C_5Me_5), 190.3, 140.7 (Ti—CH═CHPh), 124.7−143.2 (Ph). Elemental Anal. (%) Calcd for $C_{36}H_{45}NOTi_2$ (603.48): C, 71.65; H, 7.52; N, 2.32. Found: C, 71.97; H, 7.07; N, 2.74.

Preparation of [{Ti(η^5-C_5Me_5)Me(NC(Me)*t*Bu)}$_2$(μ-O)] (9). In a 100 mL J-Young Carious tube, a solution of **1** (0.200 g, 0.45 mmol) and *t*BuCN (0.078 g, 0.92 mmol) was prepared in 20 mL of toluene. The mixture was heated and stirred at 90 °C for 4 days. The solution was then filtered, concentrated to half volume, and cooled to −35 °C to give a yellow crystalline solid identified as **9** (0.211 g, 77%). The ^{1}H NMR revealed the presence of a mixture of two isomers in a ca. 1:5 ratio. IR (KBr, cm^{-1}): $\bar{\nu}$ = 2961, 2909 (s, CH aliph.), 1474, 1432, 1375, 1361, 1024 (m, CC), 1674 (vs, C═N), 772 (vs, Ti—O—Ti). ^{1}H NMR (C_6D_6, 300 MHz, 298 K): major isomer, δ = 0.44 (s, 6H, Ti—Me), 1.09 (s, 18H, N═CMe*tBu*), 1.97 (s, 30H, C_5Me_5), 1.91 (s, 6H, NCMe*t*Bu); minor isomer, δ = 0.50 (s, 6H, Ti—Me), 1.10 (s, 18H, N═CMe*tBu*), 1.96 (s, 30H, C_5Me_5), 1.89 (s, 6H, NCMe*t*Bu). ^{13}C{^{1}H} NMR (C_6D_6, 75 MHz, 298 K): major isomer, δ = 12.0 (C_5Me_5), 25.1 (NCMe*t*Bu), 28.5, 44.1 (N═CMe*tBu*), 36.1 (TiMe), 119.1 (C_5Me_5), 183.0 (N═CMe*t*Bu); minor isomer, δ = 12.0 (C_5Me_5), 25.0 (NCMe*t*Bu), 28.4, not observed (N═CMe*tBu*), 37.7 (TiMe), 119.0 (C_5Me_5), 182.6 (N═C*Me*tBu). Elemental Anal. (%) Calcd for $C_{34}H_{60}N_2OTi_2$ (608.58): C, 67.10; H, 9.94; N, 4.60. Found: C, 67.78; H, 9.33; N, 4.54.

Preparation of [{Ti(η^5-C_5Me_5)Me(NC(Me)*i*Pr)}$_2$(μ-O)] (10). Similarly, to the preparation of **9**, complex **1** (0.300 g, 0.68 mmol) and *i*PrCN (0.097 g, 1.36 mmol) were dissolved in 20 mL of hexane. The yellowish-brown solution was stirred and heated at 90 °C for 8 days. After that, the solution was filtered, its volume reduced under vacuum, and cooled to −35 °C to obtain yellowish orange crystals identified as **10** (0.249 g, 63%). The ^{1}H NMR revealed the presence of a mixture of two isomers in a ca. 1:5 ratio. IR (KBr, cm^{-1}): $\bar{\nu}$ = 2958, 2908 (s, CH aliph.), 1453 (s, CC), 1429, 1373 (m, CC), 1088 (w, CC), 1680 (vs, C═N), 781 (vs, Ti—O—Ti). ^{1}H NMR (C_6D_6, 300 MHz, 298 K): major isomer, δ = 0.50 (s, 6H, Ti—Me), 1.00, 1.04 (d, ^3J = 6.9 Hz, 6H, CH*MeMe*), 1.83 (s, 6H, N═C*Mei*Pr), 1.97 (s, 30H, C_5Me_5), 2.28 (m, ^3J = 6.9 Hz, 2H, C*H*Me$_2$); minor isomer, δ = 0.46 (s, 6H, Ti—Me), 0.99, 1.05 (d, J = 6.9 Hz, 6H, CH*MeMe*), 1.85 (s, 6H, N═C*Mei*Pr), 1.98 (s, 30H, C_5Me_5), 2.28 (m, J = 6.9 Hz, 2H, C*H*Me$_2$). ^{13}C{^{1}H} NMR (C_6D_6, 75 MHz, 298 K): major isomer, δ = 12.0 (C_5Me_5), 20.5, 20.6 (CH*MeMe*), 27.3 (N═C*Mei*Pr), 36.9 (TiMe), 41.6 (CHMe$_2$), 119.1 (C_5Me_5), 180.9 (N═C*Mei*Pr); minor isomer, δ = 11.9 (C_5Me_5), 20.6, overlapped (CH*MeMe*), 27.4 (N═C*Mei*Pr), 35.5 (TiMe), not observed (CHMe$_2$), 119.2 (C_5Me_5), 181.2 (N═C*Mei*Pr). Elemental Anal. (%) Calcd for $C_{32}H_{56}N_2OTi_2$ (580.53): C, 66.21; H, 9.72; N, 4.83. Found: C, 66.97; H, 8.50; N, 4.74.

Preparation of [{Ti(η^5-C_5Me_5)(CH_2Ph)$_2$}(μ-O){Ti(η^5-C_5Me_5)(═N(*t*Bu)C═CHPh)(NC*t*Bu)}] (11). *t*BuCN (0.023 g, 0.27 mmol) was added to a solution of **2** (0.100 g, 0.13 mmol) in 20 mL of toluene placed in a 100 mL J-Young Carious tube. The reaction mixture was stirred and heated at 65 °C for 3 days. The resultant red solution was then filtered and dried under reduced pressure to give **11** as a red microcrystalline solid (0.083 g, 75%). IR (KBr, cm^{-1}): $\bar{\nu}$ = 2911 (s, CH aliph.), 2256 (w, CN) 1483, 1377, 1205, 1160 (m, CC), 1026 (w, CC), 749 (vs, Ti—O—Ti). ^{1}H NMR (C_6D_6, 300 MHz, 298 K): δ = 0.77 (s, 9H, NC*tBu*), 1.26 (s, 9H, Ti═N—C(*tBu*)═CHPh), 1.85, 2.10 (s, 15H, C_5Me_5), 2.74, 2.65 (AB syst., 2H, ^2J = 9.9 Hz, CH_2Ph), 3.19, 2.66 (AX syst., 2H, ^2J = 9.9 Hz, CH_2Ph), 5.62 (s, 1H, Ti═N—C(*t*Bu)═C*H*Ph), 7.94−6.62 (15H, Ph). ^{13}C{^{1}H} NMR (C_6D_6, 75 MHz, 298 K): δ = 11.9, 12.2 (C_5Me_5), 32.2 (NC*tBu*), 40.5 (Ti═N—C(*tBu*)═CHPh), 71.3, 75.3 (CH$_2$Ph), 106.2 (Ti═N—C(*t*Bu)═*C*HPh), 123.9 (Ti═N—C(*t*Bu)═CHPh), 120.1, 122.1 (C_5Me_5), 121.5−150.3 (Ph), 167.7 (NC*t*Bu). Elemental Anal. (%) Calcd for $C_{51}H_{68}N_2OTi_2$ (820.83): C, 74.63; H, 8.35; N, 3.41. Found: C, 74.17; H, 7.95; N, 3.67.

Preparation of [{Ti(η^5-C_5Me_5)(CH_2Ph)$_2$}(μ-O){Ti(η^5-C_5Me_5)(═N(*i*Pr)C═C(CHPh))(NC*i*Pr)}] (12). In a similar fashion to compound **11**, in a 100 mL J-Young Carious tube, complex **2** (0.100 g, 0.13 mmol) was dissolved in 20 mL of hexane, and *i*PrCN (0.020 g, 0.28 mmol) was added. The red solution was heated and stirred at 65 °C for 4 days. After that, the solution was filtered, and the solvent was removed under reduced pressure to yield **12** (0.010 g, 10%) as a dark red microcrystalline solid. IR (KBr, cm^{-1}): $\bar{\nu}$ = 2910 (s, CH aliph.), 2266 (w, CN), 1449, 1377 (m, CC), 1274, 1024 (w, CC), 1194 (m, CC), 755 (vs, Ti—O—Ti). Elemental Anal. (%) Calcd for $C_{49}H_{64}N_2OTi_2$ (792.78): C, 74.24; H, 8.14; N, 3.53. Found: C, 73.97; H, 8.26; N, 3.81.

Preparation of [{Ti(η^5-C_5Me_5)Me_2}(μ-O){Ti(η^5-C_5Me_5)(κ^2-C,N-Me_2CNSiMe_3)(CNSiMe_3)}] (13). A 50 mL-Schlenk was charged with **1** (0.200 g, 0.45 mmol) and filled up within 10 mL of hexane, and Me_3SiCN (0.092 g, 0.904 mmol) was added. The reaction mixture was left stirring overnight at temperatures below 20 °C, and the color changed slowly from yellow to green. The solution was then filtered, concentrated to half volume, and cooled to −35 °C to give a dark green crystalline solid identified as **13** (0.226 g, 78%). IR (KBr, cm^{-1}): $\bar{\nu}$ = 2953 (s, CH aliph.), 2908 (vs, CH aliph.), 2063 (s, CN), 1436, 1377, 1080 (m, CC), 1042 (s, CC), 836, 787 (vs, Ti—O—Ti). ^{1}H NMR (C_6D_6, 300 MHz, 298 K): δ = 0.14 (s, 9H, CNSiMe_3), 0.29, 0.30 (s, 3H, TiMe), 0.52 (s, 9H, κ^2-C,N—Me_3SiNCMe$_2$), 1.32, 1.85 (s, 3H, κ^2-C,N—Me_3SiNC*MeMe*), 1.88, 1.99 (s, 15H, C_5Me_5). Elemental Anal. (%) Calcd for $C_{32}H_{60}N_2OSi_2Ti_2$ (640.73): C, 59.98; H, 9.44; N, 4.37. Found: C, 60.34; H, 8.83; N, 4.98.

Crystal Structure Determination of Complexes 3−6, 8, 9, and 11−13. All single crystals were obtained from saturated hexane solutions cooled at −35 °C. Crystals were coated with mineral oil, mounted on Mitegen MicroMounts with the aid of a microscope, and immediately placed in the low-temperature nitrogen stream of the diffractometer. The intensity data sets were collected at 200 K on a Bruker-Nonius KappaCCD diffractometer equipped with graphite-monochromated Mo Kα radiation (λ = 0.710 73 Å) and an Oxford Cryostream 700 unit. Crystallographic data are presented in Table S1 for all complexes in the Supporting Information.

The structures were solved, by using the WINGX package,[95] by direct methods (SHELXS-2013)[96] or intrinsic phasing (SHELXT-2014 for compound **4**),[97] and refined by least-squares against F^2 (SHELXL-2014).[98] All the nonhydrogen atoms were refined anisotropically. Hydrogen atoms for all the structures were positioned geometrically and refined by using a riding model, except those of complex **8** involved in the reaction, which were localized in a difference Fourier map and isotropically refined.

Crystals of **6** presented the existence of two crystallographically independent molecules, together with two disordered hexane molecules. Unfortunately, all attempts to obtain a sensible chemical model for the solvent failed, and the SQUEEZE procedure was applied to remove their contribution to the structure factors.[99]

Finally, a twin law was found for complex **3** by the ROTAX program,[100] with a refined value of 0.32 for the BASF parameter.

Computational Details. All Calculations were performed with the Gaussian16 suite of programs[101] within the framework of the density functional theory (DFT).[82,83] Electronic structure calculations were performed using the PBE0 density functional[84−86] with the D3 version of Grimme's dispersion with Becke−Johnson damping.[87] Geometry optimizations were performed by computing analytical energy gradients using the Def2-SV(P) basis set.[88,89] The obtained minima were characterized by performing energy second derivatives, confirming them as minima by the absence of negative eigenvalues of the Hessian matrix of the energy. Transition states were characterized

https://doi.org/10.1021/acs.organomet.1c00300
Organometallics 2021, 40, 2610−2623

by a single imaginary frequency, whose normal mode corresponded to the expected motion. To further refine the energies obtained from the PBE0-D3(BJ)/Def2-SV(P) calculations, single-point calculations were performed using the larger triple-ζ Def2-TZVP basis set.[88] To determine ΔG^0 values, computed electronic energies obtained using the larger basis set were corrected for zero point energy, thermal energy, and entropic effects estimated from the normal-mode analysis using the smaller basis set.

Moreover, to test the influence of the functional and basis set used in the calculations, analogous calculations were performed with the B3LYP[102,103] density functional or optimizing the structures with a larger basis set (Def2-TZVP) for Ti for some selected species as can be seen in Table S6 in the Supporting Information. Likewise, single-point calculations in toluene or hexane solution using the integral equation formalism version of the polarizable continuum model[104−106] on the previously optimized gas phase structures were finally carried out to simulate solvation effects (see Table S6 in the Supporting Information).

■ ASSOCIATED CONTENT

Supporting Information

The Supporting Information is available free of charge at https://pubs.acs.org/doi/10.1021/acs.organomet.1c00300.

All computed molecule Cartesian coordinates in a format for convenient visualization (XYZ)

Experimental data for the X-ray diffraction studies, molecular structures together with selected values for lengths (Å) and angles (deg), C−H···π interactions and parameters found for these interactions, different mechanism analysis of the reactions, Gibbs energy for different transition states, and NMR spectra (PDF)

Accession Codes

CCDC 2046469−2046477 contain the supplementary crystallographic data for this paper. These data can be obtained free of charge via www.ccdc.cam.ac.uk/data_request/cif, or by emailing data_request@ccdc.cam.ac.uk, or by contacting The Cambridge Crystallographic Data Centre, 12 Union Road, Cambridge CB2 1EZ, UK; fax: +44 1223 336033.

■ AUTHOR INFORMATION

Corresponding Author

Cristina Santamaría − *Departamento de Química Orgánica y Química Inorgánica, Instituto de Investigación Química "Andrés M. del Río" (IQAR), Universidad de Alcalá, Campus Universitario, Alcalá de Henares E-28805 Madrid, Spain*; Email: cristina.santamaria@uah.es

Authors

María Gómez-Pantoja − *Departamento de Química Orgánica y Química Inorgánica, Instituto de Investigación Química "Andrés M. del Río" (IQAR), Universidad de Alcalá, Campus Universitario, Alcalá de Henares E-28805 Madrid, Spain*

Juan I. González-Pérez − *Departamento de Química Orgánica y Química Inorgánica, Instituto de Investigación Química "Andrés M. del Río" (IQAR), Universidad de Alcalá, Campus Universitario, Alcalá de Henares E-28805 Madrid, Spain*

Avelino Martín − *Departamento de Química Orgánica y Química Inorgánica, Instituto de Investigación Química "Andrés M. del Río" (IQAR), Universidad de Alcalá, Campus Universitario, Alcalá de Henares E-28805 Madrid, Spain*

Miguel Mena − *Departamento de Química Orgánica y Química Inorgánica, Instituto de Investigación Química "Andrés M. del Río" (IQAR), Universidad de Alcalá, Campus Universitario, Alcalá de Henares E-28805 Madrid, Spain*

Manuel Temprado − *Departamento de Química Analítica, Química Física e Ingeniería Química, Instituto de Investigación Química "Andrés M. del Río" (IQAR), Universidad de Alcalá, Campus Universitario, Alcalá de Henares E-28805 Madrid, Spain*; orcid.org/0000-0002-2003-4588

Complete contact information is available at: https://pubs.acs.org/10.1021/acs.organomet.1c00300

Notes

The authors declare no competing financial interest.

■ ACKNOWLEDGMENTS

Financial support for this work was provided by the Ministerio de Ciencia, Innovación y Universidades (PGC2018-094007-B-I00). J.I.G.-P. thanks the Universidad de Alcalá for a predoctoral fellowship.

■ REFERENCES

(1) Durfee, L. D.; Rothwell, I. P. Chemistry of η^2-Acyl, η^2-Iminoacyl, and Related Functional Groups. *Chem. Rev.* **1988**, *88*, 1059−1079.

(2) Scott, M. J.; Lippard, S. J. Isocyanide Insertion Reactions with Organometallic Group 4 Tropocoronand Complexes: Formation of η^2-Iminoacyl, Enediamido, η^2-Imine, and μ-Imido Products. *Organometallics* **1997**, *16*, 5857−5868.

(3) Boyarskiy, V. P.; Bokach, N. A.; Luzyanin, K. V.; Kukushkin, V. Y. Metal-Mediated and Metal-Catalyzed Reactions of Isocyanides. *Chem. Rev.* **2015**, *115*, 2698−2779.

(4) Michelin, R. A.; Mozzon, M.; Bertani, R. Reactions of transition metal-coordinated nitriles. *Coord. Chem. Rev.* **1996**, *147*, 299−338.

(5) Chamberlain, L. R.; Durfee, L. D.; Fanwick, P. E.; Kobriger, L. M.; Latesky, S. L.; McMullen, A. K.; Steffey, B. D.; Rothwell, I. P.; Folting, K.; Huffman, J. Intramolecular Coupling of η^2-Iminoacyl and η^2-Acyl Functions at Group 4 and Group 5 Metal Centers: Structure and Spectroscopic Properties of the Resulting Enamidolate and Enediamide Complexes. *J. Am. Chem. Soc.* **1987**, *109*, 6068−6076.

(6) Durfee, L. D.; McMullen, A. K.; Rothwell, I. P. Intramolecular Coupling of η^2-Iminoacyl Groups at Group 4 Metal Centers: A Kinetic Study of the Carbon-Carbon Double-Bond-Forming Reaction. *J. Am. Chem. Soc.* **1988**, *110*, 1463−1467.

(7) Giannini, L.; Caselli, A.; Solari, E.; Floriani, C.; Chiesi-Villa, A.; Rizzoli, C.; Re, N.; Sgamellotti, A. Organometallic Reactivity on a Calix[4]arene Oxo Surface. The Stepwise Migratory Insertion of Carbon Monoxide and Isocyanides into Zirconium-Carbon Bonds Anchored to a Calix[4]arene Moiety. *J. Am. Chem. Soc.* **1997**, *119*, 9709−9719.

(8) Hardesty, J. H.; Albright, T. A.; Kahlal, S. Theoretical Investigation of Electrocyclic Ring Closure Reactions in Bis(aryloxy)-bis(η^2-iminoacyl)zirconium and Isoelectronic Complexes. *Organometallics* **2000**, *19*, 4159−4168.

(9) Ong, T.-G.; Wood, D.; Yap, G. P. A.; Richeson, D. S. Transformations of Aryl Isocyanide on Guanidinate-Supported Organozirconium Complexes To Yield Terminal Imido, Iminoacyl, and Enediamido Ligands. *Organometallics* **2002**, *21*, 1−3.

(10) Ong, T.-G.; Yap, G. P. A.; Richeson, D. S. Redefining the Coordination Geometry and Reactivity of Guanidinate Complexes by Covalently Linking the Guanidinate Ligands. Synthesis and Reactivity of [RN{NH(R)}CN$(CH_2)_2$NC{NH(R)}NR]M$(CH_2Ph)_2$(R = *i*Pr; M = Ti, Zr). *Organometallics* **2003**, *22*, 387−389.

(11) De Angelis, F.; Sgamellotti, A.; Re, N.; Fantacci, S. Intramolecular Coupling of η^2-Iminoacyls on Zirconium Bis-(aryloxides) and Calix[4]arenes: Revised Mechanism by DFT Calculations and Car-Parrinello Molecular Dynamics Simulations. *Organometallics* **2005**, *24*, 1867−1875.

(12) Fernández-Galán, R.; Antiñolo, A.; Carrillo-Hermosilla, F.; López-Solera, I.; Otero, A.; Serrano-Laguna, A.; Villaseñor, E. Migratory Insertion Reactions in Asymmetrical Guanidinate-Supported Zirconium Complexes. *Organometallics* **2012**, *31*, 8360−8369.
(13) Chiu, K. W.; Jones, R. A.; Wilkinson, G.; Galas, A. M. R.; Hursthouse, M. B. Interaction of t-Butyl lsocyanide with Methyl Compounds of Tungsten, Rhenium, Zirconium, Titanium, and Tantalum. The X-Ray Crystal Structures of W-N(Bu^t)CMe^2(Me)-(NBu^t) [N(Bu^t)CMe═CMe$_2$] and its Hydrogen Chloride Adduct. t-Butyl lsocyanide Complexes of Molybdenum(0), Ruthenium(II), and Rhodium(I). *J. Chem. Soc., Dalton Trans.* **1981**, 2088−2097.
(14) Chamberlain, L. R.; Steffey, B. D.; Rothwell, I. P.; Huffman, J. C. Synthesis and Intramolecular Coupling of Tantalum η^2-Iminoacyl (η^2-RNCR') and η^2-Imine (η^2-RNCR$_2$') Functional Groups. *Polyhedron* **1989**, *8*, 341−349.
(15) Galakhov, M. V.; Gómez, M.; Jiménez, G.; Royo, P. Insertion of Isocyanides into Tantalum-Carbon Bonds of Azatantalacyclopropane Complexes. Crystal Structures of TaCp*Cl$_3$(η^2-NRCMe$_2$CNHR), TaCp*Me(NR)(NRCMe = CMe$_2$), and TaCp*Me(NR)(η^2-NR = CCMe$_2$CMe = NR) (R = 2,6-Me$_2$C$_6$H$_3$). *Organometallics* **1995**, *14*, 2843−2854.
(16) Thomson, R. K.; Schafer, L. L. Synthesis, Structure, and Insertion Reactivity of Zirconium and Hafnium Amidate Benzyl Complexes. *Organometallics* **2010**, *29*, 3546−3555.
(17) Bercaw, J. E.; Davies, D. L.; Wolczanski, P. T. Reactions of Alkyl and Hydride Derivatives of Permethylscandocene and -zirconocene with Nitriles and Amines. Catalytic Hydrogenation of tert-Butyl Cyanide with Permethylscandocene Hydride. *Organometallics* **1986**, *5*, 443−450.
(18) Richeson, D. S.; Mitchell, J. F.; Theopold, K. H. Synthesis and Reaction Chemistry of Paramagnetic Chromium(III) Alkyls. Characterization of Complexes Formed by Insertion of Nitriles into the Chromium-Carbon Bond. *Organometallics* **1989**, *8*, 2570−2577.
(19) Bolton, P. D.; Feliz, M.; Cowley, A. R.; Clot, E.; Mountford, P. Ti = NR vs Ti-R' Functional Group Selectivity in Titanium Imido Alkyl Cations from an Experimental Perspective. *Organometallics* **2008**, *27*, 6096−6110.
(20) Hessen, B.; Blenkers, J.; Teuben, J. H.; Helgesson, G.; Jagner, S. C,C Couplings in the Reactions of Unsaturated Group 4 Metal,-cis-Butadiene Complexes with 2,6-Xylyl Isocyanide. *Organometallics* **1989**, *8*, 830−835.
(21) Martín, A.; Mena, M.; Pellinghelli, M. A.; Royo, P.; Serrano, R.; Tiripicchio, A. Some Insertion Reactions into the Ti-Me bond of [Ti(η^5-C$_5$Me$_5$)MeCl$_2$]; Crystal Structures of [Ti(η^5-C$_5$Me$_5$)(η^2-COMe)Cl$_2$] and [{Ti(η^5-C$_5$Me$_5$)}$_2$(μ-Cl)$_2${μ-η^4-CH$_2$(2,6-Me$_2$C$_6$H$_3$N) C = C(NC$_6$H$_3$Me$_2$-2,6)CH$_2$}]. *J. Chem. Soc., Dalton Trans.* **1993**, 2117−2122.
(22) Visser, C.; van den Hende, J. R.; Meetsma, A.; Hessen, B.; Teuben, J. H. Pentamethylcyclopentadienyl Zirconium and Hafnium Polyhydride Complexes: Synthesis, Structure, and Reactivity. *Organometallics* **2001**, *20*, 1620−1628.
(23) Takenaka, Y.; Hou, Z. Lanthanide Terminal Hydride Complexes Bearing Two Sterically Demanding C$_5$Me$_4$SiMe$_3$ Ligands. Synthesis, Structure, and Reactivity. *Organometallics* **2009**, *28*, 5196−5203.
(24) Li, S.; Wang, M.; Liu, B.; Li, L.; Cheng, J.; Wu, Ch; Liu, D.; Liu, J.; Cui, D. Lutetium-Methanediide-Alkyl Complexes: Synthesis and Chemistry. *Chem. - Eur. J.* **2014**, *20*, 15493−15498.
(25) Gómez-Sal, M. P.; Mena, M.; Royo, P.; Serrano, R. Structural and chemical aspects of electron deficient pentamethylcyclopentadienyltitanium halides, alkyls, and oxides. *J. Organomet. Chem.* **1988**, *358*, 147−159.
(26) Gómez-Sal, P.; Mena, M.; Palacios, F.; Royo, P.; Serrano, R.; Martínez-Carreras, S. Preparation of the compounds (nnnnnnnn-O)[Ti(C$_5$Me$_5$)R$_2$]$_2$ (R = Me, CH$_2$Ph, or CH$_2$SiMe$_3$) and the crystal structure of the derivative with R = CH$_2$SiMe$_3$. *J. Organomet. Chem.* **1989**, *375*, 59−65.
(27) Varkey, S. P.; Schormann, M.; Pape, T.; Roesky, H. W.; Noltemeyer, M.; Herbst-Irmer, R.; Schmidt, H.-G. *Inorg. Chem.* **2001**, *40*, 2427−2429.
(28) Carbó, J. J.; García-López, D.; Gómez-Pantoja, M.; González-Pérez, J. I.; Martín, A.; Mena, M.; Santamaría, C. Intermetallic Cooperation in C-H Activation Involving Transient Titanium-Alkylidene Species: A Synthetic and Mechanistic Study. *Organometallics* **2017**, *36*, 3076−3083.
(29) Groom, C. R.; Bruno, I. J.; Lightfoot, M. P.; Ward, S. C. The Cambridge Structural Database. *Acta Crystallogr., Sect. B: Struct. Sci., Cryst. Eng. Mater.* **2016**, *B72*, 171−179.
(30) Pyykkö, P.; Atsumi, M. Molecular Double-Bond Covalent Radii for Elements Li-E112. *Chem. - Eur. J.* **2009**, *15*, 12770−12779.
(31) Fandos, R.; Otero, A.; Rodríguez, A. M.; Suizo, S. Monocyclopentadienyl titanium complexes supported by functionalized Shiff Base ligands. *J. Organomet. Chem.* **2014**, *759*, 74−82.
(32) Fandos, R.; Gallego, B.; Otero, A.; Rodríguez, A.; Ruiz, M. J.; Terreros, P.; Pastor, C. A new titanium building block for early-late heterometallic complexes; preparation of a new tetrameric metallomacrocycle by self-assembly. *Dalton Trans.* **2006**, 2683−2690.
(33) Trunkely, E. F.; Epshteyn, A.; Zavalij, P. Y.; Sita, L. R. Synthesis, Structural Characterization, and Preliminary Reactivity Profile of a Series of Monocyclopentadienyl, Monoacetamidinate Titanium(III) Alkyl Complexes Bearing β-Hydrogens. *Organometallics* **2010**, *29*, 6587−6593.
(34) Xu, T.; Gao, W.; Mu, Y.; Ye, L. Synthesis and characterization of a novel η^2-iminoacyl monocyclopentadienyl titanium(IV) complex. *J. Coord. Chem.* **2007**, *60*, 2533−2539.
(35) Chiu, K. W.; Jones, R. A.; Wilkinson, G.; Galas, A. M. R.; Hursthouse, M. B. Reaction of tert-Butyl Isocyanide with Hexamethyltungsten. Synthesis and X-ray Crystal Structure of WN(But)CMe$_2$(Me)(NBut){N(But)(CMe = CMe$_2$)}. *J. Am. Chem. Soc.* **1980**, *102*, 7978−7979.
(36) Chamberlain, L. R.; Rothwell, I. P.; Huffman, J. C. Reactivity of Tantalum η^2-lminoacyl Groups: Intramolecular Coupling, Reduction, and Dealkylation. *J. Chem. Soc., Chem. Commun.* **1986**, 1203−1205.
(37) Galakhov, M. V.; Gómez, M.; Jiménez, G.; Pellinghelli, M. A.; Royo, P.; Tiripicchio, A. Insertion of CNAr into Ta-Me Bonds of TaCp*Cl$_n$Me$_{4-n}$ (n = 0−3): Intramolecular Rearrangements, Dynamic Behavior, and X-ray Crystal Structure of TaCp*Cl$_2$(NAr) (Ar = 2,6-Me$_2$C$_6$H$_3$). *Organometallics* **1994**, *13*, 1564−1566.
(38) Xiang, L.; Mashima, K.; Xie, Z. Reaction of [η^1:η^5-(Me$_2$NCH$_2$CH$_2$)C$_2$B$_9$H$_{10}$]TaMe$_3$ with aryl isonitriles: tantallacarborane-mediated facile cleavage of C-N multiple bonds. *Chem. Commun.* **2013**, *49*, 9039−9041.
(39) Matsuo, Y.; Mashima, K.; Tan, K. Intramolecular Coupling Reaction of 1-Aza-1,3-butadiene Ligand and Iminoacyl Ligand Giving Amido-Imido Complexes of Tantalum. *Organometallics* **2002**, *21*, 138−143.
(40) Basuli, F.; Bailey, B. C.; Tomaszewski, J.; Huffman, J. C.; Mindiola, D. J. A Terminal and Four-Coordinate Titanium Alkylidene Prepared by Oxidatively Induced (-Hydrogen Abstraction. *J. Am. Chem. Soc.* **2003**, *125*, 6052−6053.
(41) Figueroa, J. S.; Piro, N. A.; Mindiola, D. J.; Fickes, M. G.; Cummins, C. C. Niobaziridine Hydrides. *Organometallics* **2010**, *29*, 5215−5229.
(42) Xiang, J.; Xie, Z. Reaction of [η^1:η^5-(R$_2$NCH$_2$CH$_2$)C$_2$B$_9$H$_{10}$]-TaMe$_3$ with Isonitriles: Effects of Nitrogen Substituents on Product Formation. *Organometallics* **2016**, *35*, 1430−1439.
(43) Ziegler, J. A.; Bergman, R. G.; Arnold, J. Unusual κ1 coordination of a β-diketiminate ligand in niobium complexes. *Dalton Trans.* **2016**, *45*, 12661−12668.
(44) Gómez-Pantoja, M.; González-Pérez, J. I.; Martín, A.; Mena, M.; Santamaría, C.; Temprado, M. Reactivity of tuck-over titanium oxo complexes with isocyanides. *Organometallics* **2018**, *37*, 2046−2053.
(45) March, J.; Smith, M. B. *March's Advanced Organic Chemistry Reactions, Mechanism, and Structure*, 5th ed.; John Wily & Sons: New York, 2001.

https://doi.org/10.1021/acs.organomet.1c00300
Organometallics 2021, 40, 2610−2623

(46) Zhang, S.; Piers, E. W. Methane Loss from Cationic μ-Methyl Dimers Formed via Trityl Borate Activation of Monocyclopentadienyl Ketimide Complexes Cp[(^{t}Bu)$_2$C = N]Ti(CH$_3$)$_2$ (Cp = C$_5$H$_5$, C$_5$Me$_5$, C$_5$Me$_4$SiMe$_3$). *Organometallics* **2001**, *20*, 2088−2092.
(47) Bochmann, M.; Wilson, L. M.; Hursthouse, M. B.; Motevall, M. Insertion Reactions of Nitriles in Cationic Alkylbis(cyclopentadienyl) titanium Complexes: The Facile Synthesis of Azaalkenylidene Titanium Complexes and the Crystal and Molecular Structure of [(Indenyl)$_2$Ti(NCMePh)(NCPh)]BPh$_4$. *Organometallics* **1988**, *7*, 1148−1154.
(48) Ferreira, M. J.; Matos, I.; Ascenso, J. R.; Duarte, M. T.; Marques, M. M.; Wilson, C.; Martins, A. M. Alkylation, Cation Formation, and Insertion Reactions in Titanium Tris(ketimide) Complexes. *Organometallics* **2007**, *26*, 119−127.
(49) Latham, A. A.; Leigh, G. J. The Chemistry of Dinitrogen Residues. Part 1. Diazenido-complexes of Titanium, and some Substituted Analogues. X-Ray Crystal Structures of [Ti(C$_5$H$_5$)-Cl$_2$(NNPh)], [Ti(C$_5$H$_5$)Cl$_2$(NCBu^{n}Bu^t)], and [Ti(C$_5$H$_5$)-Cl$_2$(NPPh,)]. *J. Chem. Soc., Dalton Trans.* **1986**, 377−383.
(50) Dias, A. R.; Duarte, M. T.; Fernandes, A. C.; Fernandes, S.; Marques, M. M.; Martins, A. M.; da Silva, J. F.; Rodrigues, S. S. Titanium ketimide complexes as α-olefin homo- and copolymerisation catalysts. X-ray diffraction structures of [TiCp'(N = C^{t}Bu$_2$)Cl$_2$] (Cp' = Ind, Cp*). *J. Organomet. Chem.* **2004**, *689*, 203−213.
(51) Nomura, K.; Yamada, J.; Wang, W.; Liu, J. Effect of ketimide ligand for ethylene polymerization and ethylene/norbornene copolymerization catalyzed by (cyclopentadienyl)(ketimide)titanium complexes-MAO catalyst systems: Structural analysis for Cp*TiCl$_2$(N = CPh$_2$). *J. Organomet. Chem.* **2007**, *692*, 4675−4682.
(52) Carbó, J. J.; García-López, D.; González-del Moral, O.; Martín, A.; Mena, M.; Santamaría, C. Carbon-Nitrogen Bond Construction and Carbon-Oxygen Double Bond Cleavage on a Molecular Titanium Oxonitride: A Combined Experimental and Computational Study. *Inorg. Chem.* **2015**, *54*, 9401−9412.
(53) Haehnel, M.; Ruhmann, M.; Theilmann, O.; Roy, S.; Beweries, T.; Arndt, P.; Spannenberg, A.; Villinger, A.; Jemmis, E. D.; Schulz, A.; Rosenthal, U. Reactions of Titanocene Bis(trimethylsilyl)acetylene Complexes with Carbodiimides: An Experimental and Theoretical Study of Complexation versus C-N Bond Activation. *J. Am. Chem. Soc.* **2012**, *134*, 15979−15991.
(54) Selby, J. D.; Manley, C. D.; Feliz, M.; Schwarz, A. D.; Clot, E.; Mountford, P. New ligand platforms for developing the chemistry of the Ti = N-NR$_2$ functional group and the insertion of alkynes into the N-N bond of a Ti = N-NPh$_2$ ligand. *Chem. Commun.* **2007**, 4937−4939.
(55) Schofield, A. D.; Nova, A.; Selby, J. D.; Schwarz, A. D.; Clot, E.; Mountford, P. Reaction Site Diversity in the Reactions of Titanium Hydrazides with Organic Nitriles, Isonitriles and Isocyanates: Ti = N$_\alpha$ Cycloaddition, Ti = N$_\alpha$ Insertion and N$^\alpha$-N$^\beta$ Bond Cleavage. *Chem. - Eur. J.* **2011**, *17*, 265−285.
(56) Scheffler, U.; Stosser, R.; Mahrwald, R. Retropinacol/Cross-Pinacol Coupling Reactions - A Catalytic Access to 1,2-Unsymmetrical Diols. *Adv. Synth. Catal.* **2012**, *354*, 2648−2652.
(57) Gauch, E.; Hoppe, H.; Strähle, J. Syntheses and structures of di- and trinuclear heterometallic complexes with nitrido bridges between rhenium and titanium. *J. Organomet. Chem.* **2000**, *593*−*594*, 175−179.
(58) Basuli, F.; Bailey, B. C.; Watson, L. A.; Tomaszewski, J.; Huffman, J. C.; Mindiola, D. J. Four-Coordinate Titanium Alkylidene Complexes: Synthesis, Reactivity, and Kinetic Studies Involving the Terminal Neopentylidene Functionality. *Organometallics* **2005**, *24*, 1886−1906.
(59) Seckar, J. A.; Thayer, J. S. Normal-Iso Rearrangement in Cyanotrialkylsilanes. *Inorg. Chem.* **1976**, *15*, 501−504.
(60) Galakhov, M. V.; Gómez, M.; Jiménez, G.; Royo, P.; Pellinghelli, M. A.; Tiripicchio, A. Synthesis and Dynamic Behavior of (Pentamethylcyclopentadieny1) azatantalacyclopropane Complexes. Crystal Structures of TaCp*Cl$_4$[C(Me)(NHR)] and TaCp*Me$_2$(η^2-Me$_2$CNR). *Organometallics* **1995**, *14*, 1901−1910.
(61) Gómez, M.; Gómez-Sal, P.; Jiménez, G.; Martín, A.; Royo, P.; Sánchez-Nieves, J. Insertion of CO and CNR into Tantalum-Methyl Bonds of Imido(pentamethylcyclopentadienyl)tantalum Complexes. X-ray Crystal Structures of [TaCp*(NR)Me{η^2-C(Me)=NR}] and [TaCp*Cl(O){η^2-C(Me)=NR}] (R = 2,6-Me$_2$C$_6$H$_3$). *Organometallics* **1996**, *15*, 3579−3587.
(62) Boring, E.; Sabat, M.; Finn, M. G.; Grimes, R. N. Insertion Reactions of Tantalum(V) Carborane Alkyl and Aryl Complexes with Nitriles and Isonitriles. Thermal and Photochemical Isomerization of η^2-Iminoacyl Isomers. *Organometallics* **1997**, *16*, 3993−4000.
(63) Thorn, M. G.; Fanwick, P. E.; Rothwell, I. P. Reactivity of Group 4 Metal Alkyl and Metallacyclic Compounds Supported by Aryloxide Ligands Toward Organic Isocyanides. *Organometallics* **1999**, *18*, 4442−4447.
(64) Matsuo, Y.; Mashima, K.; Tani, K. Intramolecular Coupling Reaction of 1-Aza-1,3-butadiene Ligand and Iminoacyl Ligand Giving Amido-Imido Complexes of Tantalum. *Organometallics* **2002**, *21*, 138−143.
(65) Valadez, T. N.; Norton, J. R.; Neary, M. C. Reaction of Cp*(Cl)M(Diene) (M = Ti, Hf) with Isonitriles. *J. Am. Chem. Soc.* **2015**, *137*, 10152−10155.
(66) González-Pérez, J. I.; Martín, A.; Mena, M.; Santamaría, C. C-H Activation on an Oxo-Bridged Dititanium Complex: From Alkyl to aaaaaaaa-Alkylidene Functionalities. *Organometallics* **2016**, *35*, 2488−2493.
(67) Santamaría, C.; Beckhaus, R.; Haase, D.; Koch, R.; Saak, W.; Strauss, I. Reactions of the Titanaallene Intermediate [Cp*$_2$Ti = C=CH$_2$] with Isonitriles: An Approach to the Chemistry of Radialene Type Molecules. *Organometallics* **2001**, *20*, 1354−1359.
(68) Carofiglio, T.; Floriani, C.; Chiesi-Villa, A.; Guastini, C. Isocyanide Complexes of Titanium(1V) and Vanadium(V): Concerning the Nonexistent Insertion of Isocyanides into a Metal-Chloride Bond. *Inorg. Chem.* **1989**, *28*, 4417−4419.
(69) Carofiglio, T.; Cozzi, P. G.; Floriani, C.; Chiesi-Villa, A.; Rizzoli, C. Nonorganometallic Pathway of the Passerini Reaction Assisted by Titanium Tetrachloride. *Organometallics* **1993**, *12*, 2726−2736.
(70) Hahn, F. E.; Lügger, T. Isocyanide complexes of titanium: synthesis and X-ray crystal structure of cis-tetrachlorobis(2-trimethylsiloxyphenylisocyanide)titanium(IV). *J. Organomet. Chem.* **1995**, *501*, 341−346.
(71) Durfee, L. D.; Hill, J. E.; Fanwick, P. E.; Rothwell, I. P. Formation and Characterization of η^2-Imine and η^2-Azobenzene Derivatives of Titanium Containing Ancillary Aryloxide Ligation. *Organometallics* **1990**, *9*, 75−80.
(72) Hill, J. E.; Balaich, G.; Fanwick, P. E.; Rothwell, I. P. The Chemistry of Titanacyclopentadiene Rings Supported by 2,6-Diphenylphenoxide Ligation: Stoichiometric and Catalytic Reactivity. *Organometallics* **1993**, *12*, 2911−2924.
(73) Steinhuebel, D. P.; Lippard, S. J. Synthesis and Characterization of (Aminotroponiminato)titanium(IV) Dialkyl Complexes: Control of Reactivity by Ligand Design. *Organometallics* **1999**, *18*, 3959−3961.
(74) Tomaszewski, R.; Arif, A. M.; Ernst, R. D. Tandem couplings of imines and other unsaturated organic compounds with a half-open titanocene. *J. Chem. Soc., Dalton Trans.* **1999**, 1883−1890.
(75) Adler, C.; Bekurdts, A.; Haase, D.; Saak, W.; Schmidtmann, M.; Beckhaus, R. Bulky Titanium Amides: C-H Bond Activation under Mild Conditions. *Eur. J. Inorg. Chem.* **2014**, *2014*, 1289−1302.
(76) Fandos, R.; Fernández-Gallardo, J.; López-Solera, M. I.; Otero, A.; Rodríguez, A.; Ruiz, M. J.; Terreros, P. Preparation, Characterization, and Reactivity of Tantalum Complexes Containing Tridentate Bis(phenolato) [OSO]-Type Ligands. *Organometallics* **2008**, *27*, 4803−4809.
(77) Xiang, L.; Xie, Z. Tantallacarborane Mediated Consecutive C-C and C-N Coupling Reactions of Alkyl Isonitriles: A Facile Route to N-Heterocycles. *Organometallics* **2016**, *35*, 233−241.

https://doi.org/10.1021/acs.organomet.1c00300
Organometallics 2021, 40, 2610−2623

(78) Nakamoto, K. *Infrared and Raman Spectra of Inorganic and Coordination Compounds, Part A Theory and Applications in Inorganic Chemistry*; Wiley-Interscience: New York, 1997; Vol 2.
(79) Dunn, S. C.; Hazari, N.; Cowley, A. R.; Green, J. C.; Mountford, P. Synthesis and Reactions of Group 4 Imido Complexes Supported by Cyclooctatetraene Ligands. *Organometallics* **2006**, *25*, 1755−1770.
(80) Floriani, C.; Corazza, F.; Lesueur, W.; Chiesi-Villa, A.; Guastini, C. A Sensitive Spectroscopic Probe for Monitoring Changes in the Coordination Sphere of Titanium: Eight-Membered Dioxatitanacycles and Their Organometallic Derivative. *Angew. Chem., Int. Ed. Engl.* **1989**, *28*, 66−67.
(81) Unruangsri, J.; Morgan, H.; Schwarz, A. D.; Schofield, D.; Mountford, P. Synthesis and Reactivity of Titanium Hydrazido Complexes Supported by Diamido-Ether Ligands. *Organometallics* **2013**, *32*, 3091−3107.
(82) Hohenberg, P.; Kohn, W. Inhomogeneus Electron Gas. *Phys. Rev.* **1964**, *136*, B864−B871.
(83) Kohn, W.; Sham, L. J. Self-Consistent Equations Including Exchange and Correlation Effects. *Phys. Rev.* **1965**, *140*, A1133−A1138.
(84) Perdew, J. P.; Burke, K.; Ernzerhof, M. Generalized Gradient Approximation Made Simple. *Phys. Rev. Lett.* **1996**, *77*, 3865−3868.
(85) Perdew, J. P.; Burke, K.; Ernzerhof, M. Generalized Gradient Approximation. *Phys. Rev. Lett.* **1997**, *78*, 1396.
(86) Adamo, C.; Barone, V. Toward reliable density functional methods without adjustable parameters: The PBE0 model. *J. Chem. Phys.* **1999**, *110*, 6158−6170.
(87) Ernzerhof, M.; Scuseria, G. E. Assessment of the Perdew-Burke-Ernzerhof exchange-correlation functional. *J. Chem. Phys.* **1999**, *110*, 5029−5036.
(88) Grimme, S.; Ehrlich, S.; Goerigk, L. Effect of the Damping Function in Dispersion Corrected Density Functional Theory. *J. Comput. Chem.* **2011**, *32*, 1456−1465.
(89) Weigend, F.; Ahlrichs, R. Balanced basis sets of split valence, triple zeta valence and quadruple zeta valence quality for H to Rn: Design and assessment of accuracy. *Phys. Chem. Chem. Phys.* **2005**, *7*, 3297−3305.
(90) Thorn, M. G.; Lee, J.; Fanwick, P. E.; Rothwell, I. P. Synthesis, structure and molecular dynamics of η^2-iminoacyl compounds [Cp(ArO)Zr(η^2-Bu^{t}NCCH$_2$Ph)(CH$_2$Ph)] and [Cp(ArO)Zr(η^2-ButNCCH$_2$Ph)$_2$]. *J. Chem. Soc., Dalton Trans.* **2002**, 3398−3405.
(91) Galájov, M.; García, C.; Gómez, M.; Gómez-Sal, P.; Temprado, M. Synthesis and DFT, Multinuclear Magnetic Resonance, and Xmray Structural Studies of Iminoacyl Imido Hydridotris(3,5-dimethylpyrazolyl)borate Niobium and Tantalum(V) Complexes. *Organometallics* **2014**, *33*, 2277−2286.
(92) Chen, J.; Chen, T.; Norton, J. R.; Rauch, M. Insertion of Isonitriles into the Zr-CH$_3$ Bond of Cp*$_2$Zr(CH$_3$)$_2$ and Electrophilic Cleavage of the Remaining Methyl Group. *Organometallics* **2018**, *37*, 4424−4430.
(93) Bailey, B. C.; Fout, A. R.; Fan, H.; Tomaszewski, J.; Huffman, J. C.; Gary, J. B.; Johnson, M. J. A.; Mindiola, D. J. Snapshots of an Alkylidyne for Nitride Triple-Bond Metathesis. *J. Am. Chem. Soc.* **2007**, *129*, 2234−2235.
(94) It is worth mentioning that minimum **I6** is 1.4 kcal mol^{-1} more stable than transition state **TS$_{ISI7}$** in terms of electronic energy at 0 K; however, thermal energy and entropic effects surmount this small electronic energy difference and revert the expected trend in Gibbs energy at 25 °C, as can be seen in Figure 8.
(95) Farrugia, L. J. WinGX and ORTEP for Windows: an update. *J. Appl. Crystallogr.* **2012**, *45*, 849−854.
(96) Sheldrick, G. M. A short history of SHELX. *Acta Crystallogr., Sect. A: Found. Crystallogr.* **2008**, *A64*, 112−122.
(97) Sheldrick, G. M. SHELXT-Integrated space-group and crystal-structure determination. *Acta Crystallogr., Sect. A: Found. Adv.* **2015**, *71*, 3−8.
(98) Sheldrick, G. M. Crystal structure refinement with SHELXL. *Acta Crystallogr., Sect. C: Struct. Chem.* **2015**, *C71*, 3−8.
(99) Spek, A. L. PLATON SQUEEZE: a tool for the calculation of the disordered solvent contribution to the calculated structure factors. *Acta Crystallogr., Sect. C: Struct. Chem.* **2015**, *C71*, 9−18.
(100) Cooper, R. I.; Gould, R. O.; Parsons, S.; Watkin, D. J. The derivation of non-merohedral twin laws during refinement by analysis of poorly fitting intensity data and the refinement of non-merohedrally twinned crystal structures in the program CRYSTALS. *J. Appl. Crystallogr.* **2002**, *35*, 168−174.
(101) Frisch, M. J.; Trucks, G. W.; Schlegel, H. B.; Scuseria, G. E.; Robb, M. A.; Cheeseman, J. R.; Scalmani, G.; Barone, V.; Petersson, G. A.; Nakatsuji, H.; Li, X.; Caricato, M.; Marenich, A. V.; Bloino, J.; Janesko, B. G.; Gomperts, R.; Mennucci, B.; Hratchian, H. P.; Ortiz, J. V.; Izmaylov, A. F.; Sonnenberg, J. L.; Williams-Young, D.; Ding, F.; Lipparini, F.; Egidi, F.; Goings, J.; Peng, B.; Petrone, A.; Henderson, T.; Ranasinghe, D.; Zakrzewski, V. G.; Gao, J.; Rega, N.; Zheng, G.; Liang, W.; Hada, M.; Ehara, M.; Toyota, K.; Fukuda, R.; Hasegawa, J.; Ishida, M.; Nakajima, T.; Honda, Y.; Kitao, O.; Nakai, H.; Vreven, T.; Throssell, K.; Montgomery, J. A., Jr.; Peralta, J. E.; Ogliaro, F.; Bearpark, M.; Heyd, J. J.; Brothers, E. N.; Kudin, K. N.; Staroverov, V. N.; Kobayashi, R.; Normand, J.; Raghavachari, K.; Rendell, A.; Burant, J. C.; Iyengar, S. S.; Tomasi, J.; Cossi, M.; Millam, J. M.; Klene, M.; Adamo, C.; Cammi, R.; Ochterski, J. W.; Martin, R. L.; Morokuma, K.; Farkas, O.; Foresman, J. B.; Fox, D. J. *Gaussian 16*, revision B.01; Gaussian, Inc.: Wallingford CT, 2016.
(102) Becke, A. D. Density-functional thermochemistry. III. The role of exact exchange. *J. Chem. Phys.* **1993**, *98*, 5648−5652.
(103) Lee, C.; Yang, W.; Parr, R. G. Development of the Colle-Salvetti correlation-energy formula into a functional of the electron density. *Phys. Rev. B: Condens. Matter Mater. Phys.* **1988**, *37*, 785−789.
(104) Miertuš, S.; Scrocco, E.; Tomasi, J. Electrostatic interaction of a solute with a continuum. A direct utilization of AB initio molecular potentials for the prevision of solvent effects. *Chem. Phys.* **1981**, *55*, 117−129.
(105) Tomasi, J.; Mennucci, B.; Cammi, R. Quantum Mechanical Continuum Solvation Models. *Chem. Rev.* **2005**, *105*, 2999−3094.
(106) Scalmani, G.; Frisch, M. J. Continuous surface charge polarizable continuum models of solvation. I. General formalism. *J. Chem. Phys.* **2010**, *132*, 114110.

https://doi.org/10.1021/acs.organomet.1c00300
Organometallics 2021, 40, 2610−2623